

Manuscript Number:	GIGA-D-19-00092
Full Title:	Assessment of human diploid genome assembly with 10x Linked-Reads data
Article Type:	Data Note
Funding Information:	
Abstract:	<p>Background: Producing cost-effective haplotype-resolved personal genomes remains challenging. 10x Linked-Read sequencing, with its high base quality and long-range information, has been demonstrated to facilitate de novo assembly of human genomes and variant detection. In this study, we investigate in depth how the parameter space of 10x library preparation and sequencing affects assembly quality, on the basis of both simulated and real libraries.</p> <p>Findings: We prepared and sequenced eight 10x libraries with a diverse set of parameters from standard cell lines NA12878 and NA24385 and performed whole genome assembly on the data. We also developed the simulator LRTK-SIM to follow the workflow of 10x data generation and produce realistic simulated Linked-Read data sets. We found that assembly quality could be improved by increasing the total sequencing coverage (C) and keeping physical coverage of DNA fragments (CF) or read coverage per fragment (CR) within broad ranges. The optimal physical coverage was between 332X and 823X and assembly quality worsened if it increased to greater than 1,000X for a given C. Long DNA fragments could significantly extend phase blocks, but decreased contig contiguity. The optimal length-weighted fragment length ($W\mu_FL$) was around 50 – 150kb. When broadly optimal parameters were used for library preparation and sequencing, ca. 80% of the genome was assembled in a diploid state.</p> <p>Conclusion: The Linked-Read libraries we generated and the parameter space we identified provide theoretical considerations and practical guidelines for personal genome assemblies based on 10x Linked-Read sequencing.</p> <p>Keywords: 10x Linked-Read sequencing, de novo assembly, diploid human genome, library preparation</p>
Corresponding Author:	arend sidow UNITED STATES
Corresponding Author Secondary Information:	
Corresponding Author's Institution:	
Corresponding Author's Secondary Institution:	
First Author:	Lu Zhang
First Author Secondary Information:	
Order of Authors:	Lu Zhang Xin Zhou Ziming Weng arend sidow
Order of Authors Secondary Information:	
Additional Information:	
Question	Response
Are you submitting this manuscript to a special series or article collection?	No

<p>Experimental design and statistics</p> <p>Full details of the experimental design and statistical methods used should be given in the Methods section, as detailed in our Minimum Standards Reporting Checklist. Information essential to interpreting the data presented should be made available in the figure legends.</p> <p>Have you included all the information requested in your manuscript?</p>	<p>Yes</p>
<p>Resources</p> <p>A description of all resources used, including antibodies, cell lines, animals and software tools, with enough information to allow them to be uniquely identified, should be included in the Methods section. Authors are strongly encouraged to cite Research Resource Identifiers (RRIDs) for antibodies, model organisms and tools, where possible.</p> <p>Have you included the information requested as detailed in our Minimum Standards Reporting Checklist?</p>	<p>Yes</p>
<p>Availability of data and materials</p> <p>All datasets and code on which the conclusions of the paper rely must be either included in your submission or deposited in publicly available repositories (where available and ethically appropriate), referencing such data using a unique identifier in the references and in the “Availability of Data and Materials” section of your manuscript.</p> <p>Have you have met the above requirement as detailed in our Minimum Standards Reporting Checklist?</p>	<p>Yes</p>

[Click here to view linked References](#)

1 **Assessment of human diploid genome assembly with 10x**

2 **Linked-Reads data**

3 **Lu Zhang^{1,2,3,*}, Xin Zhou^{3,*}, Ziming Weng², Arend Sidow^{2,4,†}**

4 ¹Department of Computer Science, Hong Kong Baptist University

5 ²Department of Pathology, Stanford University

6 ³Department of Computer Science, Stanford University

7 ⁴Department of Genetics, Stanford University

8 *These authors contributed equally to this work. †Correspondence and requests for materials should be
9 addressed to Arend Sidow (email: arend@stanford.edu)

10 **Abstract**

11 **Background:** Producing cost-effective haplotype-resolved personal genomes remains
12 challenging. 10x Linked-Read sequencing, with its high base quality and long-range information,
13 has been demonstrated to facilitate *de novo* assembly of human genomes and variant detection.
14 In this study, we investigate in depth how the parameter space of 10x library preparation and
15 sequencing affects assembly quality, on the basis of both simulated and real libraries.

16 **Findings:** We prepared and sequenced eight 10x libraries with a diverse set of parameters from
17 standard cell lines NA12878 and NA24385 and performed whole genome assembly on the data.
18 We also developed the simulator LRTK-SIM to follow the workflow of 10x data generation and
19 produce realistic simulated Linked-Read data sets. We found that assembly quality could be
20 improved by increasing the total sequencing coverage (C) and keeping physical coverage of DNA
21 fragments (C_F) or read coverage per fragment (C_R) within broad ranges. The optimal physical
22 coverage was between 332X and 823X and assembly quality worsened if it increased to greater
23 than 1,000X for a given C . Long DNA fragments could significantly extend phase blocks, but
24 decreased contig contiguity. The optimal length-weighted fragment length ($W\mu_{FL}$) was around 50
25 – 150kb. When broadly optimal parameters were used for library preparation and sequencing, ca.
26 80% of the genome was assembled in a diploid state.

27 **Conclusion:** The Linked-Read libraries we generated and the parameter space we identified
28 provide theoretical considerations and practical guidelines for personal genome assemblies
29 based on 10x Linked-Read sequencing.

30 **Keywords:** 10x Linked-Read sequencing, *de novo* assembly, diploid human genome, library
31 preparation

32 **Data description**

33 **Introduction**

34 The human genome holds the key for understanding the genetic basis of human evolution,
35 hereditary illnesses and many phenotypes. Whole-genome reconstruction and variant discovery,
36 accomplished by analysis of data from whole-genome sequencing experiments, are foundational
37 for the study of human genomic variation and analysis of genotype-phenotype relationships. Over
38 the past decades, cost-effective whole-genome sequencing has been revolutionized by short-
39 fragment approaches, the most widespread of which have been the consistently improving
40 generations of the original Solexa technology [1, 2], now referred to as Illumina sequencing.
41 Illumina's strengths and weaknesses are inherent in the sample prep and sequencing chemistry.
42 Illumina generates short paired reads (2x150 base pairs for the highest-throughput platforms)
43 from short fragments (usually 400-500 base pairs) [3]. Because many clonally amplified molecules
44 generate a robust signal during the sequencing reaction, Illumina's average per-base error rates
45 are very low.

46

47 The lack of long-range contiguity between end-sequenced short fragments limits their application
48 for reconstructing personal genomes. Long-range contiguity is important for phasing variants and
49 dealing with genomic complex regions. For haplotyping, variants can be phased by population-
50 based methods [4, 5] or family-based recombination inference [6, 7], but such approaches are
51 only feasible for common variants or large pedigrees. Furthermore, highly polymorphic regions
52 such as the HLA in which the reference sequence does not adequately capture the diversity
53 segregating in the population are refractory to mapping-based approaches and require *de novo*
54 assembly to reconstruct [8]. Short-read/short-fragment data are challenged by interspersed
55 repetitive sequences from mobile elements and by segmental duplications, and only support
56 highly fragmented genome reconstruction [9, 10].

57

58 In principle, many of these challenges can be overcome by long-read/long-fragment sequencing
59 [11, 12]. Assembly of Pacific Biosciences (PacBio) or Oxford Nanopore (ONT) data can yield
60 impressive contiguity of contigs and scaffolds. In one study, scaffold N50 reached 31.1Mb by
61 hierarchically integrating PacBio long reads and BioNano for a hybrid assembly, which also
62 uncovered novel tandem repeats and replicated the structural variants that were newly included
63 in the updated hg38 human reference sequence. Another study [13] produced human genome
64 assemblies with ONT data, in which a contig N50 ~3Mb was achieved, and long contigs covered
65 all class I HLA regions. However, long-fragment sequencing suffers from low throughput, high
66 cost, and low base quality, hampering its usefulness for personal genome assembly.

67

68 Hierarchical assembly pipelines in which multiple data types are used [14] as another approach.
69 For example, in the reconstruction of an Asian personal genome, fosmid clone pools and Illumina
70 data were merged, but because fosmid libraries are highly labor intensive to generate and
71 sequence, this approach is not generalizable to personal genomes. The "Long Fragment Read"
72 (LFR) approach, where a long fragment is sequenced at high depth via single-molecule
73 fragmented amplification, reported promising personal genome assembly and variant phasing by
74 attaching a barcode to the short reads derived from the same long fragment. However, because
75 LFR is implemented in a 384 well plate, many long fragments would be labelled by the same
76 barcodes, making it difficult for binning short-reads, and the great sequencing depth required
77 rendered LFR not cost-effective.

78

79 An alternative approach is offered by the 10x Genomics Chromium system, which distributes the
80 DNA prep into millions of partitions where partition-specific barcode sequences are attached to
81 short amplification products that are templated off the input fragments. Because of the limited
82 reaction efficiency in each partition, the sequencing depth for each fragment is too shallow to

83 reconstruct the original long-fragment, distinguishing this approach from LFR [15]. However, to
84 compensate for the low read coverage of each fragment, each genomic region is covered by
85 hundreds of DNA fragments, giving overall sequence coverage that is in a range comparable to
86 standard Illumina short-fragment sequencing while providing very high physical coverage. Novel
87 computational approaches leveraging the special characteristics of 10x Genomics data have
88 already generated significant advances in power and accuracy of haplotyping [16, 17], cancer
89 genome reconstruction [18, 19], metagenomic assemblies [20], and *de novo* assembly of human
90 and other genomes [21-23], compared to standard Illumina short-fragment sequencing. While the
91 uniformity of sequence coverage is not as good as with PCR-free Illumina libraries, 10x Linked-
92 Read sequencing is a promising technology that combines low per-base error and good small-
93 variant discovery with long-range information for much improved SV detection in mapping-based
94 approaches [19, 24], and the possibility of long-range contiguity in *de novo* assembly [21, 23, 25].
95
96 Practical advantages of the technology include the low DNA input mass requirement (1ng per
97 library, or approximately 300 haploid human genome equivalents). Real input quantities can vary,
98 along with other factors, to influence an interconnected array of parameters that are relevant to
99 genome assembly and reconstruction. The parameters over which the experimenter has influence
100 are (**Figure 1**): i). C_R : average Coverage of short Reads per fragment; ii). C_F : average physical
101 Coverage of the genome by long DNA Fragments; iii). $N_{F/P}$: Number of Fragments per Partition;
102 iv). Fragment length distribution, several parameters of which are used, specifically μ_{FL} : Average
103 Unweighted DNA Fragment Length and $W\mu_{FL}$: Length-Weighted average of DNA Fragment
104 Length. Note that several parameters depend on each other. For example, a greater amount of
105 input DNA will increase $N_{F/P}$; shorter fragments increase $N_{F/P}$ at the same DNA input amount
106 compared to longer fragments; less input DNA will (within practical constraints) increase C_R and
107 decrease C_F ; and their absolute values are set by how much total sequence coverage is
108 generated because $C_R \times C_F = C$.

109

110 Our goal in this study was to experimentally explore the 10x parameter space and evaluate the
111 quality of *de novo* diploid assembly as a function of the parameter values. For example, we set
112 out to ask whether longer input fragments produce better assemblies, or what the effect of
113 sequencing vs. physical coverage is on contiguity of assembly. In order to constrain the parameter
114 space, we first performed computer simulations with reasonably realistic synthetic data. The
115 simulation results suggested certain parameter combinations that we then approximated in the
116 generation of real, high-depth, sequence data on two human reference genome cell lines,
117 NA12878 and NA24385. These simulated and real data sets were then used to produce *de novo*
118 assemblies, with an emphasis on the performance of 10x's Supernova2 [21]. We finally assessed
119 the quality of the assemblies using standard metrics of contiguity and accuracy, facilitated by the
120 existence of a gold standard (in the case of simulations) and comparisons to the reference
121 genome (in the case of real data).

122

123 **Library preparation, physical parameters and sequencing coverage**

124 We made six DNA preparations that varied in fragment size distribution and amount of input DNA,
125 three each from NA12878 and NA24385. From these, we prepared eight libraries, five from
126 NA12878 and three from NA24385 (**Table S1**). To generate library L_{1L} , L_{1M} and L_{1H} , genomic
127 DNA was extracted from ca. 1 million cultured NA12878 cells using the Gentra Puregene Blood
128 Kit following manufacturer's instructions (Qiagen, Cat. No 158467). The GEMs were divided into
129 3 tubes with 5%, 20%, and 75% to generate libraries L_{1L} , L_{1M} and L_{1H} , respectively (**Figure S1-**
130 **S3**). For the other libraries, to generate longer DNA fragments ($W_{\mu_{FL}}=150\text{kb}$ and longer, **Figure**
131 **S4-S8**), a modified protocol was applied. Two-hundred thousand NA12878 or NA24385 cells of
132 fresh culture were added to 1mL cold 1x PBS in a 1.5 ml tube and pelleted for 5 minutes at 300g.
133 The cell pellets were completely resuspended in the residual supernatant by vortexing and then

134 lysed by adding 200ul Cell Lysis Solution and 1ul of RNaseA Solution (Qiagen, Cat. No 158467),
135 mixing by gentle inversion, and incubating at 37°C for 15-30 minutes. This cell lysis solution is
136 used immediately as input for the 10x Chromium prep (Chromium™ Genome Library & Gel Bead
137 Kit v2, PN-120258; Chromium™ i7 Multiplex Kit, PN-120262). Fragment size of the input DNA
138 can be controlled by gentle handling during lysis and DNA preparation for Chromium. The amount
139 of input DNA (between 1.25 and 4 ng) was varied to achieve a wide range of physical coverage
140 (C_F). The Chromium Controller was operated and the GEM prep was performed as instructed by
141 the manufacturer. Individual libraries were then constructed by end repairing, A-tailing, adapter
142 ligation and PCR amplification. All libraries were sequenced with three lanes of paired-end 150bp
143 runs on the Illumina HiSeqX to obtain very high coverage ($C=94x-192x$), though the two with the
144 fewest number of gel beads (L_{1L} and L_{1M}) exhibited high PCR duplication rates because of the
145 reduced complexity of the libraries (**Table S1**).

146

147 **Linked-Reads subsampling**

148 The high sequencing coverage in the libraries allowed subsampling to facilitate the matching of
149 parameters among the different libraries, for purposes of comparability; these subsampled
150 Linked-Read sets are denoted R_{id} (**Figure 1**). We aligned the 10x Linked-Reads to human
151 reference genome (hg38) followed by removing PCR duplication by barcode-aware analysis in
152 Long Ranger[18]. Original input DNA fragments were inferred by collecting the read-pairs with the
153 same barcode that were aligned in proximity to each other. A fragment was terminated if the
154 distance between two consecutive reads with the identical barcode larger than 50kb. Fragments
155 were required to have at least two read pairs with the same barcode and a length of at least 2 kb.
156 Partitions with fewer than three fragments were removed. We subsampled short-reads for each
157 fragment to satisfy the expected C_R .

158

159 **Generating 10x simulated libraries by LRTK-SIM**

160 To compare the observations from real data with a known truth set, we developed LRTK-SIM, a
161 simulator that follows the workflow of the 10x Chromium system and generates synthetic Linked-
162 Reads like those produced by an Illumina HiSeqX machine (**Supplementary Information** and
163 **Figure S9**). Based on the parameters commonly employed by 10x Genomics Linked-Read
164 sequencing and the characteristics of our libraries, LRTK-SIM generated simulated datasets from
165 the human reference (hg38), explicitly modeling the five key steps in real data generation.
166 Parameters in parentheses are from the standard 10x Genomics protocol: 1. Shearing genomic
167 DNA into long fragments ($W_{\mu_{FL}}$ from 50kb to 100kb); 2. Loading DNA to the 10x Chromium
168 instrument (~1.25ng DNA); 3. Allocating DNA fragments into partitions which are attached the
169 unique barcodes (~10 fragments per partition); 4. Generating short fragments; 5. Generating
170 Illumina paired-end short reads (800M~1200M reads). LRTK-SIM first generated a diploid
171 reference genome as a template by duplicating the human reference genome (hg38) into two
172 haplotypes and inserting SNVs from high-confidence regions in GIAB of NA12878; For low-
173 confidence regions we randomly simulated 1 SNV per 1 kb. The ratio was 2:1 for heterozygous
174 and homozygous SNVs. From this diploid reference genome, LRTK-SIM generated long DNA
175 fragments by randomly shearing each haplotype with multiple copies into pieces whose lengths
176 were sampled from an exponential distribution with mean of μ_{FL} . These fragments were then
177 allocated to pseudo-partitions, and all the fragments within each partition were assigned the same
178 barcode. The number of fragments for each partition was randomly picked from a Poisson
179 distribution with mean of $N_{F/P}$. Finally, paired-end short reads were generated according to C_R and
180 replaced the first 16bp of the reads from forward strand to the assigned barcodes followed by 7
181 Ns. More information about implementation can be found in **Supplementary Information**. From
182 that diploid genome, Linked-Read datasets were generated that varied in C_R , C_F and μ_{FL} ($W_{\mu_{FL}}$)
183 (**Table S2-S3**). Varying $N_{F/P}$ was only done for chromosome 19 because of the infeasibility of

184 running Supernova2 on whole genome assemblies with large N_{FP} ; within practically reasonable
185 values, N_{FP} does not appear to influence assembly quality (**Figure S10**). In total, we generated
186 17 simulated Linked-Read datasets to explore the overall parameter space (**Table S2-S3**) and 11
187 to match the parameters of the abovementioned real libraries (**Figure 1**).

188

189 **Human genome diploid assembly and evaluation**

190 The scaffolds were generated by the “pseudohap2” output of Supernova2, which explicitly
191 generated two haploid scaffolds, simultaneously. Contigs were generated by breaking the
192 scaffolds if at least 10 consecutive ‘N’s appeared, per definition by Supernova2. For the
193 simulations of human chromosome 19, we used the scaffolds from the “megabubbles” output.
194 Contig and scaffold N50 and NA50 were used to evaluate assembly quality. Contigs longer than
195 500bp were aligned to hg38 by Minimap2[30]. We calculated contig NA50 on the basis of contig
196 misassemblies reported by QUAST-LG [31]. For scaffolds (longer than 1kb), we calculated the
197 NA50 following Assemblathon 1's procedure [32] (**Supplementary Information**).

198

199 **Performance of diploid assembly: influence of total coverage** Diploid assembly by Linked-
200 Reads requires sufficient total read coverage ($C=C_R \times C_F$) to generate long contigs and scaffolds.
201 In this experiment, to explore the roles of both physical coverage (C_F) and per-fragment read
202 coverage (C_R), we first generated eight simulated libraries whose total coverage C ranged from
203 16x to 78x: four with C_R fixed and increasing C_F and four with fixed C_F , and increasing C_R (**Table**
204 **S2**). Contig and scaffold N50s increased along with increasing either C_F or C_R (**Figure 2A** and
205 **2B**). To investigate whether the trend was also present in the real datasets, we analyzed six real
206 libraries (three by varying C_F , and the other three by varying C_R ; **Figure 1**): as C increased, we
207 varied C_F and C_R independently by fixing the other parameter. Contig and scaffold N50s also
208 increased in in these real Linked-Read sets (**Figure 2C, 2D, 2E** and **2F**) as a function of total

209 coverage C . Contig lengths did increase but not dramatically so when C was increased beyond
210 56X. Accuracy, which we define as the ratio between NA50 (N50 after breaking contigs or
211 scaffolds at assembly errors) and N50 (**Figure 2C** and **2E**), did not change appreciably. For
212 scaffolds in the real data sets, when C increased from 48X (R_3) to 67X (R_4), both scaffold N50
213 and NA50 were significantly improved (N50: 13.4Mb to 30.6Mb; NA50: 6.3Mb to 12.0Mb), but the
214 accuracy dropped slightly from 46.6% to 39.1%, which indicated that scaffold accuracy may be
215 refractory to extremely high C (**Figure 2F**). These results indicated that assembly length and
216 accuracy were comparable over a broad range of C_F and C_R at constant C , which implied that
217 assembly quality was mainly determined by C .

218

219 **Performance of diploid assembly: influence of fragment length and physical coverage.** To
220 investigate if input weighted fragment length (as measured by $W_{\mu_{FL}}$) influenced assembly quality,
221 we generated four simulated libraries (**Table S3**) with fixed C_F and C_R and a range of fragment
222 lengths (**Figure 3A**). Contig length decreased with increasing fragment length, a trend that was
223 also seen in six real libraries (**Figure 3B**; $C=56X$; R_6 to R_{11} in **Figure 1**). We then simulated
224 another six libraries with the same parameters as the real ones to explore the effects of physical
225 coverage at constant $C=56x$ (**Figure 3C**). Contig lengths decreased as a function of increasing
226 physical coverage, a trend that is somewhat less clear in real data possibly due to confounding
227 other parameters such as fragment length (**Figure 3D**).

228

229 **Performance of diploid assembly: nature of the source genome.** Assembly errors may occur
230 because of heterozygosity, repetitive sequences, or sequencing error. To illuminate possible
231 sources of assembly error, we performed simulations by generating 10x-like Linked-Reads as
232 above from human chromosome 19, and then quantified assembly error against these synthetic
233 gold standards. Removal of interspersed repeat sequences from the source genome resulted in

234 better contigs with no loss of accuracy in experiments by varying C_F , C_R and μ_{FL} (**Figure 4A, 4C**
235 and **4E**) and better scaffolds only if C_R was above 1X (**Figure 4D**). Removal of variation had little
236 effect on contigs and only gave rise to longer scaffolds if C_R was above 0.8X (**Figure S11**), which
237 is difficult to achieve with real libraries. Finally, a 1% uniform sequencing error had no discernible
238 effect (**Figure S12**).

239

240 **Performance of diploid assembly: fraction of genome in diploid state.** While contiguity is an
241 important parameter for any whole genome assembly, evaluation of diploid assemblies
242 necessitates estimating the fraction of the genome in which the assembly recovered the diploid
243 state. To this end, we divided the contigs generated by Supernova2 into “diploid contigs”, which
244 were extracted from its megabubble structures, and “haploid contigs” from non-megabubble
245 structures. Pairs of scaffolds were extracted as the two haplotypes from megabubble structures
246 if they shared the same start and end nodes in the assembly graph. Diploid contigs were
247 generated by breaking the candidate scaffolds at the sequences with least 10 consecutive ‘N’s
248 and were aligned to human reference genome (hg38) by Minimap2. The genome was split into
249 500bp windows and diploid regions were defined as the maximum extent of successive windows
250 covered by two contigs, each from one haplotype. Alignment against the human reference
251 genome revealed the overall genome coverages of the six assemblies to be around 91%. For
252 most assemblies, 70%-80% of the genome was covered by two homologous contigs (**Table 1**),
253 with R_6 only reaching 58.9%, probably due to the short fragments of the DNA prep ($\mu_{FL}=24\text{kb}$). We
254 also analyzed another seven assemblies produced by 10x Genomics, all of which had diploid
255 fractions of about 80% as well (**Table S4**). In the male NA24385, non-pseudoautosomal regions
256 of the X chromosome are hemizygous and should therefore be recovered as haploid regions.
257 Between 79.9% and 87.6% of these regions were covered by one contig exactly depending on
258 the assembled library. Library construction parameters other than fragment length appeared to
259 have had little impact on the proportion of diploid regions (**Tables 1 and Table S4**).

260

261 Overlapping the diploid regions from the assemblies of the same individual revealed that 50.24%
262 and 67.27% of the genome for NA12878 and NA24385 (**Figure S13**), respectively, were diploid
263 in all the three assemblies. NA12878 was lower because of the low percentage of diploid regions
264 in assembly R_6 (**Table 1**). The overlaps were significantly greater than expected by chance
265 (NA12878: 33.3%, p-value=0.0049; NA24385: 45.4%, p-value=0.0029. Chi square test). These
266 observations were consistent with heterozygous variants being enriched in certain genomic
267 segments, in which two haplotypes were more easily differentiated by Supernova2. Phase block
268 lengths were mainly determined by total coverage C and increased in real data with increasing
269 fragment length (**Figure S14**).

270

271 **Discussion**

272 In this study, we investigated human diploid assembly using 10x Linked-Read sequencing data
273 on both simulated and real libraries. We developed the simulator LRTK-SIM to examine the likely
274 impact of parameters in diploid assembly and compared results from simulated reads to those
275 from real libraries. We thus determined the impact of key parameters (C_R , C_F , N_{FP} and $\mu_{FL}/N\mu_{FL}$)
276 with respect to assembly continuity and accuracy. Our study provides a general strategy to
277 evaluate assemblies of 10x data and may have implications for the evaluation of other barcode-
278 based sequencing technologies such as CPTv2-seq [26] or stLRF [27] in the future when they
279 become commercially available.

280

281 **10x Practicalities**

282 For standard Illumina sequencing, library complexity is usually sufficient to generate tremendous
283 numbers of reads from unique templates and read coverage can be increased simply by
284 sequencing more. However, the 10x Chromium system performs amplification in each partition,

285 and generally only about 20% to 40% of the original long fragment sequence can be captured as
286 short fragments and eventually as reads, resulting in shallow sequencing coverage per fragment.
287 Sequencing more deeply does not increase the per-fragment coverage much as most of the extra
288 reads are from PCR duplicates. The solution is to sequence multiple 10x libraries constructed
289 from the same DNA prep and merge them for analysis. This means that C_R remains in the
290 standard range where PCR duplicates are relatively rare, but C_F increases proportionally to the
291 number of libraries used. A practical limitation to this approach is that Supernova2 limits the
292 number of barcodes to 4.8 million.

293

294 Our results showed that in practice, C_F should be between 335X and 823X, but no larger than
295 1000X, given the optimal coverage of $C=56X$ recommended by 10x and the requirement for
296 sufficient per-fragment read coverage. Surprisingly, we observed that including more extremely
297 long fragments was detrimental for assembly quality. This is possibly due to the loss of barcode
298 specificity for fragments spanning repetitive sequences. From a computational perspective, too
299 many long fragments are harmful to deconvolving the *de bruijn* graph, as more complex paths
300 need to be picked out. In our experiments, $W_{\mu_{FL}}$ between 50kb and 150kb is the best choice to
301 generate reliable assemblies.

302

303 **Parameters driving assembly quality**

304 Our results regarding assembly quality, and the 10x parameters that influence it, may be useful
305 for efforts in which *de novo* assemblies are important for generation of an initial reference
306 sequence. We show that maximization of N50 does not necessarily reflect assembly quality,
307 which we were able to compare to NA50 because there exists a high-quality human reference
308 genome. Contig and scaffold lengths mostly increased with ascending sequencing coverage, and
309 at sufficient overall sequence coverage it did not matter much whether the increasing coverage
310 C was accomplished by increasing C_R or C_F . However, both contig and scaffold accuracy

311 decreased with increasing C . We also found, counterintuitively, that contig and scaffold length
312 mostly decreased with increasing fragment length, a phenomenon that may be due to the specific
313 implementation; however, until there is another assembler that can be compared to Supernova2
314 it will not be possible to reason about this effect. In addition, intrinsic properties of the genome
315 matter greatly, as removal of repeats or lack of variation dramatically improves assembly quality.

316

317 Diploid assembly is the appropriate approach for assembly of genomes of diploid organisms that
318 harbor variation. Therefore, an important metric to evaluate diploid assembly is the fraction of the
319 genome that is assembled in a diploid state. The short input fragment length of R_6 resulted in
320 roughly 20% less of the genome in a diploid state (<60% vs <80%) compared to the other libraries
321 of the same individual. This observation suggests that in addition to metrics such as N50,
322 evaluation of assembly quality should also include the fraction of the genome (or the assembly)
323 that is in a diploid state.

324

325 **Cost-benefit analysis**

326 Overall, we have attempted to give practical guidelines to assembly of 10x data with Supernova2
327 and evaluate the performance across a wide range of metrics. Arguably, the metric that matters
328 most in the context of a personal genome is the discovery of variation that lower-cost approaches
329 do not enable. We estimate that the cost increase over standard Illumina sequencing is about 2x,
330 given the 10X prep cost and the higher level of sequence coverage required. There may be many
331 applications for which this combination of excellent single nucleotide variant detection (via
332 barcode-aware read mapping) and precise structural variant discovery (via assembly), achieved
333 by the same data set, is worth the price.

334

335 **Comparison with hybrid assemblies**

336 Hybrid assembly strategies have been applied successfully to produce human genome assembly
337 of long contiguity [13, 28, 29]. In these studies, long contigs are first produced by single-molecule
338 long-reads, such as PacBio (NG50=1.1Mb; [28]) or Nanopore (NG50=3.21Mb; [13]) comparing
339 favorably to our best results for Linked-Reads assemblies (NG50=236kb). Scaffolding is then
340 performed with complementary technologies such as BioNano to capture chromosomal level long-
341 range information. It promoted the scaffold N50 of PacBio to 31.1Mb [28] and Illumina mate-pair
342 sequencing with 10x data to 33.5Mb [22]. Using SuperNova2, the scaffold N50 from our studies
343 reached ~27.86Mb (R_6) on the basis of 10x data alone, suggesting that 10x technology gives
344 broadly comparable results at a fraction of the price of long-read-based hybrid assemblies.

345 **Availability of supporting data**

346 The raw sequencing data are deposited in the Sequence Read Archive and the corresponding
347 BioProject accession number is PRJNA527321. Diploid assemblies and the codes for comparison
348 are currently available at http://mendel.stanford.edu/supplementarydata/zhang_SN2_2019 and
349 https://github.com/zhanglu295/Evaluate_diploid_assembly. LRTK-SIM is publicly available at
350 <https://github.com/zhanglu295/LRTK-SIM>.

351

352 **Additional files**

353 **Table S1.** Parameters of libraries prepared for NA12878 and NA24385.

354 **Table S2.** Parameters used to generate linked-reads sets for evaluating the impact of C_F and C_R
355 on assemblies.

356 **Table S3.** Parameters used to generate linked-reads sets for evaluating the impact of μ_{FL} and
357 N_{FP} on assemblies.

358 **Table S4.** Genomic coverage and fraction of contigs in diploid state generated by Supernova2
359 for the seven libraries prepared by 10x Genomics. Non-PAR: non-pseudoautosomal regions of
360 X chromosome. WFU, YOR, YORM, PR are female; HGP, ASH and CHI are male.

361 **Figure S1. Basic statistics for L_{1L} .** The distributions of **A.** the number of fragments per partition;
362 **B.** sequencing depth per fragment; **C.** probability density function of unweighted fragment lengths;
363 **D.** cumulative density function of unweighted fragment lengths; **E.** reversed cumulative density
364 function of unweighted fragment lengths; **F.** reversed cumulative density function of weighted
365 fragment lengths.

366 **Figure S2. Basic statistics for L_{1M} .** The distributions of **A.** number of fragments per partition; **B.**
367 sequencing depth per fragment; **C.** probability density function of unweighted fragment lengths;
368 **D.** cumulative density function of unweighted fragment lengths; **E.** reversed cumulative density
369 function of unweighted fragment lengths; **F.** reversed cumulative density function of weighted
370 fragment lengths.

371 **Figure S3. Basic statistics for L_{1H} .** The distributions of **A.** number of fragments per partition; **B.**
372 sequencing depth per fragment; **C.** probability density function of unweighted fragment lengths;
373 **D.** cumulative density function of unweighted fragment lengths; **E.** reversed cumulative density
374 function of unweighted fragment lengths; **F.** reversed cumulative density function of weighted
375 fragment lengths.

376 **Figure S4. Basic statistics for L_2 .** The distributions of **A.** number of fragments per partition; **B.**
377 sequencing depth per fragment; **C.** probability density function of unweighted fragment lengths;
378 **D.** cumulative density function of unweighted fragment lengths; **E.** reversed cumulative density
379 function of unweighted fragment lengths; **F.** reversed cumulative density function of weighted
380 fragment lengths.

381 **Figure S5. Basic statistics for L_3 .** The distributions of **A.** number of fragments per partition; **B.**
382 sequencing depth per fragment; **C.** probability density function of unweighted fragment lengths;
383 **D.** cumulative density function of unweighted fragment lengths; **E.** reversed cumulative density
384 function of unweighted fragment lengths; **F.** reversed cumulative density function of weighted
385 fragment lengths.

386 **Figure S6. Basic statistics for L_4 .** The distributions of **A.** number of fragments per partition; **B.**
387 sequencing depth per fragment; **C.** probability density function of unweighted fragment lengths;
388 **D.** cumulative density function of unweighted fragment lengths; **E.** reversed cumulative density
389 function of unweighted fragment lengths; **F.** reversed cumulative density function of weighted
390 fragment lengths.

391 **Figure S7. Basic statistics for L_5 .** The distributions of **A.** number of fragments per partition; **B.**
392 sequencing depth per fragment; **C.** probability density function of unweighted fragment lengths;
393 **D.** cumulative density function of unweighted fragment lengths; **E.** reversed cumulative density
394 function of unweighted fragment lengths; **F.** reversed cumulative density function of weighted
395 fragment lengths.

396 **Figure S8. Basic statistics for L_6 .** The distributions of **A.** number of fragments per partition; **B.**
397 sequencing depth per fragment; **C.** probability density function of unweighted fragment lengths;
398 **D.** cumulative density function of unweighted fragment lengths; **E.** reversed cumulative density
399 function of unweighted fragment lengths; **F.** reversed cumulative density function of weighted
400 fragment lengths.

401 **Figure S9.** The workflow of LR TK-SIM to simulate linked-reads

402 **Figure S10.** The effect of N_{FP} on human diploid assembly of chromosome 19 by Supernova2,
403 where C ($C=60X$; $C_F=300X$ and $C_R=0.2X$) and μ_{FL} ($\mu_{FL}=37\text{kb}$) are fixed.

404 **Figure S11.** Comparison of assembly qualities from 10x data with and without single nucleotide
405 variants by changing C_F , C_R and μ_{FL} . C_R was fixed to 0.2X in **A** and **B**; C_F was fixed to 300X in
406 **C** and **D**; C_R was fixed 0.2X and C_F was fixed 300X in **E** and **F**.

407 **Figure S12.** Comparison of assembly qualities from 10x data with (1% uniform) and without
408 sequencing error by changing C_F , C_R and μ_{FL} . C_R was fixed to 0.2X in **A** and **B**; C_F was fixed to
409 300X in **C** and **D**; C_R was fixed 0.2X and C_F was fixed 300X in **E** and **F**.

410 **Figure S13.** Overlaps of diploid regions for the three libraries from the same sample. Diploid
411 regions for NA12878 (**A**) and NA24385 (**B**). The percentages denote the proportion of genome is
412 diploid.

413 **Figure S14.** Phase block N50s as a function of different parameter combinations. **A.** simulated
414 linked-reads with predefined parameters (**Table S4**) by changing C_F and C_R ; **B.** simulated linked-
415 reads with matched parameters of real linked-read sets (**Table S2**) by changing C_F and C_R ; **C.**
416 real linked-read sets (**Table S2**) by changing C_F and C_R ; **D.** simulated linked-read sets (**Table S3**)
417 with different $W_{\mu_{FL}}$; **E.** simulated linked-read sets with matched parameters (**Table S3**) with real
418 linked-read sets as $C=56X$; **F.** real linked-read sets with $C=56X$ (**Table S3**).

419

420 **Competing interest**

421 Arend Sidow is a consultant and shareholder of DNAnexus, Inc.

422 **Author Contributions**

423 AS conceived the study. LZ and XZ wrote LRTK-SIM and performed the analyses. ZMW prepared
424 the genomic DNA and 10x libraries. LZ, XZ, ZMW and AS analyzed the results and wrote the
425 paper. All the authors read and approved the final manuscript.

426 **Acknowledgements**

427 This research was supported by training and research grants from the National Institute of
428 Standards and Technology. We would like to thank Justin Zook, Marc Salit, Alex Bishara, Noah
429 Spies, Nancy Hansen, David Jaffe, and Deanna Church for informative discussions.

430 **Table**

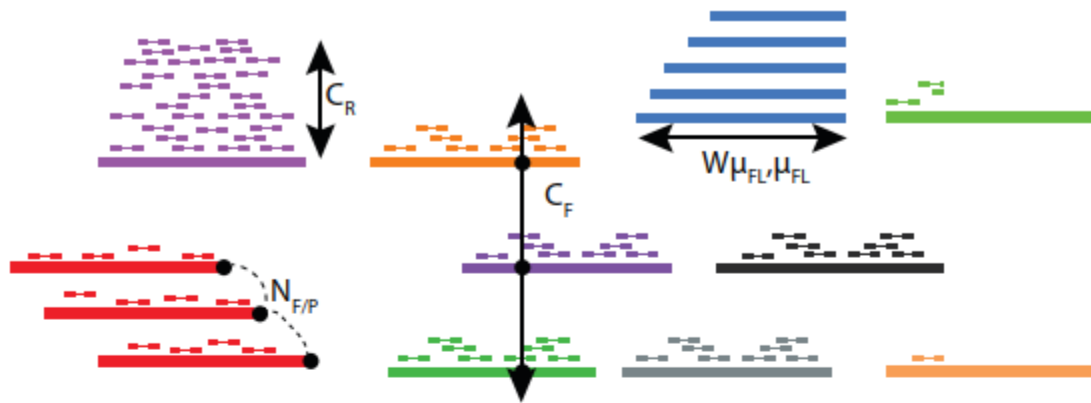
Linked- reads set	Overall (%)	Diploid regions (%)	Haploid regions (%)	Non-PAR (%)	Total contig length (contig>500bp)	Length of contigs from megabubble (contig>500bp)	Percentage (%)
R_6	91.9	58.9	27.7	-	5,632,483,053	3,758,345,846	66.73
R_7	91.1	73.3	11.3	-	5,613,140,437	4,668,186,478	83.17
R_8	91.7	77.2	9.2	-	5,635,127,471	4,896,821,850	86.90
R_9	91.3	73.4	12.2	85.9	5,637,615,919	4,438,175,621	78.72
R_{10}	91.7	79.2	5.8	79.9	5,749,001,471	4,793,226,150	83.37
R_{11}	91.7	78.1	7.9	87.6	5,677,566,094	4,723,083,367	83.19

431

432 **Table 1.** Genomic coverage of contigs generated by Supernova2. Non-PAR: non-
 433 pseudoautosomal regions of X chromosome. R_6 , R_7 and R_8 are female; R_9 , R_{10} and R_{11} are male.

434

435 **Figures**



Parameter

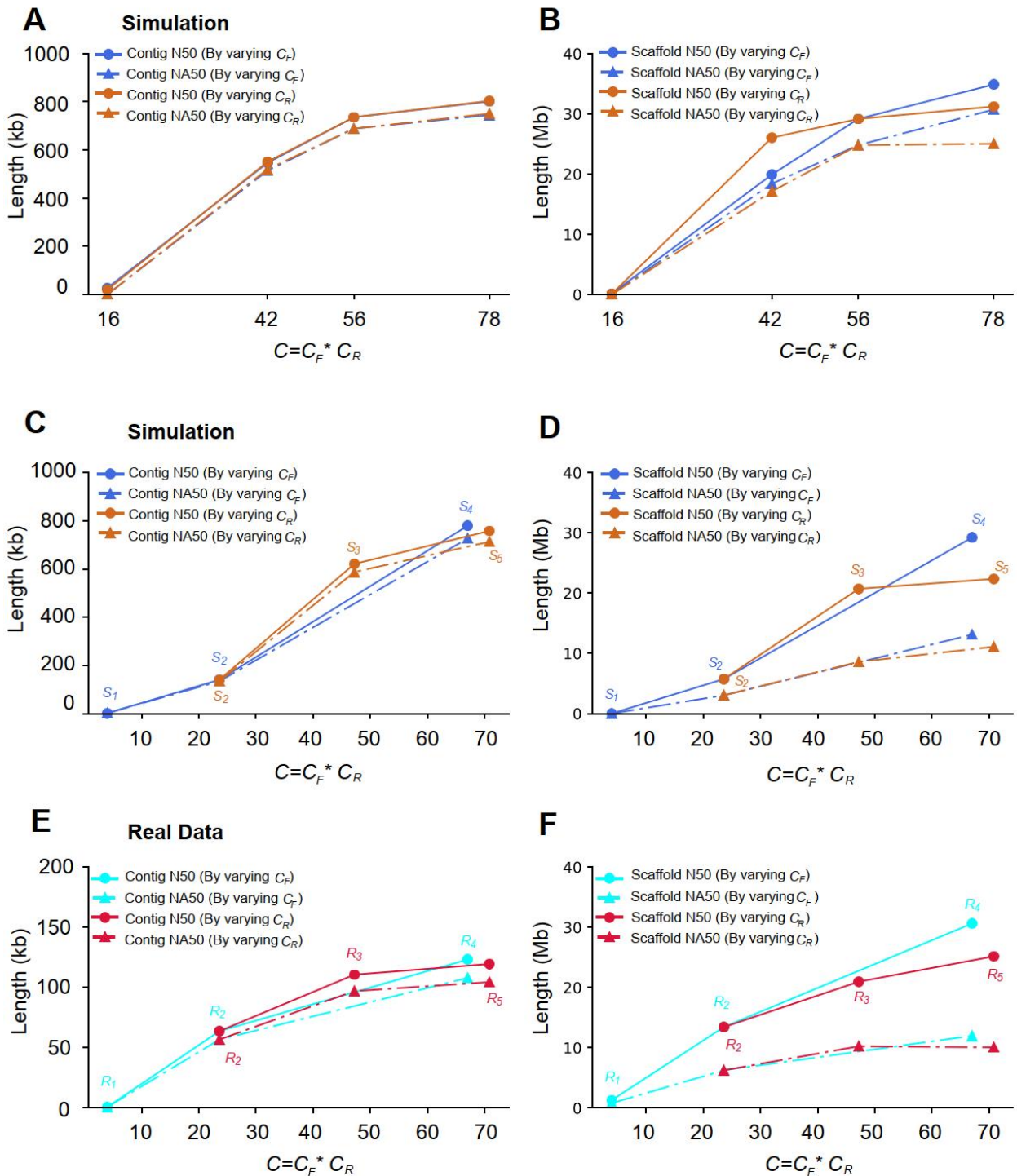
$N_{F/P}$ = Number of fragments per partition
 μ_{FL} = Mean fragment length
 $W\mu_{FL}$ = Weighted mean fragment length
 C_R = Read coverage per fragment
 C_F = Physical (fragment) coverage
 C = total coverage

Typical values

10 - 100
 μ_{FL} = 10-100kb
 $W\mu_{FL}$ = 20-400kb
 C_R = 0.1x - 0.4x
 C_F = 200x - 1000x
 $C = C_R * C_F = 40x - 80x$

Linked-read set R (Real) / S (Simulated)	Sequenced Library	μ_{FL} (kb)	$W\mu_{FL}$ (kb)	C_F (X)	C_R (X)	C (X)
R_1 / S_1	L_{1L}	21.6	38.6/35.7	19	0.2	4
R_2 / S_2	L_{1M}	22.4	39.7/37.4	117	0.2	24
R_3 / S_3	L_{1M}	22.4	39.7/36.8	117	0.4	48
R_4 / S_4	L_{1H}	24.0	41.1/40.7	334	0.2	67
R_5 / S_5	L_{1M}	22.4	39.7/36.8	117	0.6	72
R_6 / S_6	L_{1H}	24.0	41.1/40.6	334	0.17	56
R_7 / S_7	L_2	79.0	304.3/131.8	123	0.45	56
R_8 / S_8	L_3	99.2	214.5/168.3	958	0.058	56
R_9 / S_9	L_4	92.1	216.9/154.1	1504	0.036	56
R_{10} / S_{10}	L_5	120.8	267.4/203.7	208	0.27	56
R_{11} / S_{11}	L_6	64.2	151.7/107.6	803	0.07	56

436 **Figure 1.** The Linked-Read sets prepared to evaluate the impact of C_F , C_R , μ_{FL} and $W\mu_{FL}$ on
 437 human diploid assembly.

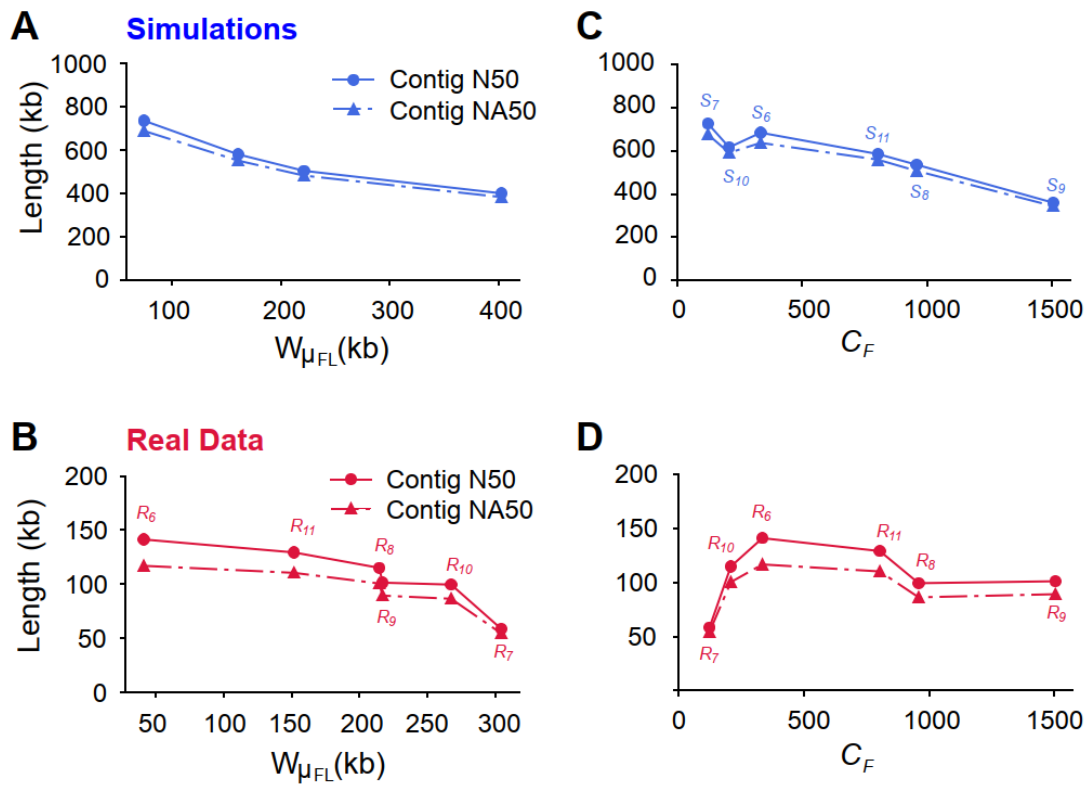


438

439 **Figure 2.** Contig and scaffold lengths (N50 and NA50) as a function of C_F or C_R . **A** and **B**:

440 Simulated Linked-Reads with predefined parameters (**Table S2**); **C** and **D**: Simulated Linked-

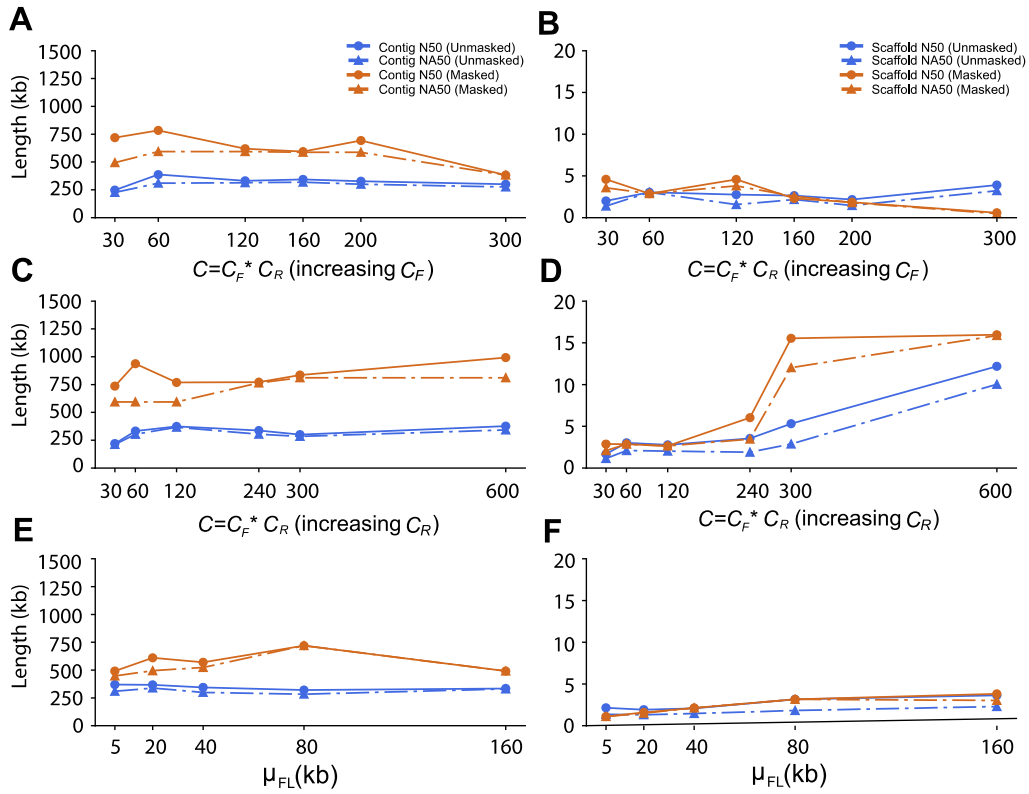
441 reads with matched parameters of real Linked-Read data sets (**Figure 1**); **E** and **F**: Real Linked-
442 Read sets (**Figure 1**).



443

444 **Figure 3.** Contig qualities (N50 and NA50) as a function of fragment length $W_{\mu_{FL}}$ or physical

445 coverage C_F , at $C=56X$. **A** and **C**, results from simulations; **B** and **D**, results from real data.



446

447 **Figure 4.** Comparison of contig and scaffold lengths from 10x data with masked and unmasked

448 repetitive sequences by changing C_F , C_R and μ_{FL} . C_R was fixed to 0.2X in **A** and **B**; C_F was fixed

449 to 300X in **C** and **D**; C_R was fixed to 0.2X and C_F was fixed to 300X in **E** and **F**.

450

451 **References**

- 452 1. Metzker ML. Sequencing technologies - the next generation. *Nat Rev Genet.* 2010;11 1:31-
453 46. doi:10.1038/nrg2626.
- 454 2. Shendure J, Balasubramanian S, Church GM, Gilbert W, Rogers J, Schloss JA, et al. DNA
455 sequencing at 40: past, present and future. *Nature.* 2017;550 7676:345-53.
456 doi:10.1038/nature24286.
- 457 3. Head SR, Komori HK, LaMere SA, Whisenant T, Van Nieuwerburgh F, Salomon DR, et
458 al. Library construction for next-generation sequencing: overviews and challenges.
459 *Biotechniques.* 2014;56 2:61-4, 6, 8, passim. doi:10.2144/000114133.
- 460 4. O'Connell J, Sharp K, Shrine N, Wain L, Hall I, Tobin M, et al. Haplotype estimation for
461 biobank-scale data sets. *Nat Genet.* 2016;48 7:817-20. doi:10.1038/ng.3583.
- 462 5. Delaneau O, Zagury JF and Marchini J. Improved whole-chromosome phasing for disease
463 and population genetic studies. *Nat Methods.* 2013;10 1:5-6. doi:10.1038/nmeth.2307.
- 464 6. O'Connell J, Gurdasani D, Delaneau O, Pirastu N, Ulivi S, Cocca M, et al. A general
465 approach for haplotype phasing across the full spectrum of relatedness. *PLoS Genet.*
466 2014;10 4:e1004234. doi:10.1371/journal.pgen.1004234.
- 467 7. Roach JC, Glusman G, Hubley R, Montsaroff SZ, Holloway AK, Mauldin DE, et al.
468 Chromosomal haplotypes by genetic phasing of human families. *Am J Hum Genet.*
469 2011;89 3:382-97. doi:10.1016/j.ajhg.2011.07.023.
- 470 8. Kajitani R, Toshimoto K, Noguchi H, Toyoda A, Ogura Y, Okuno M, et al. Efficient de
471 novo assembly of highly heterozygous genomes from whole-genome shotgun short reads.
472 *Genome Res.* 2014;24 8:1384-95. doi:10.1101/gr.170720.113.

- 473 9. Alkan C, Sajjadian S and Eichler EE. Limitations of next-generation genome sequence
474 assembly. *Nat Methods*. 2011;8 1:61-5. doi:10.1038/nmeth.1527.
- 475 10. Treangen TJ and Salzberg SL. Repetitive DNA and next-generation sequencing:
476 computational challenges and solutions. *Nat Rev Genet*. 2011;13 1:36-46.
477 doi:10.1038/nrg3117.
- 478 11. Huddleston J, Ranade S, Malig M, Antonacci F, Chaisson M, Hon L, et al. Reconstructing
479 complex regions of genomes using long-read sequencing technology. *Genome Res*.
480 2014;24 4:688-96. doi:10.1101/gr.168450.113.
- 481 12. Lu H, Giordano F and Ning Z. Oxford Nanopore MinION Sequencing and Genome
482 Assembly. *Genomics Proteomics Bioinformatics*. 2016;14 5:265-79.
483 doi:10.1016/j.gpb.2016.05.004.
- 484 13. Jain M, Koren S, Miga KH, Quick J, Rand AC, Sasani TA, et al. Nanopore sequencing and
485 assembly of a human genome with ultra-long reads. *Nat Biotechnol*. 2018;36 4:338-45.
486 doi:10.1038/nbt.4060.
- 487 14. Cao H, Wu H, Luo R, Huang S, Sun Y, Tong X, et al. De novo assembly of a haplotype-
488 resolved human genome. *Nat Biotechnol*. 2015;33 6:617-22. doi:10.1038/nbt.3200.
- 489 15. Peters BA, Kermani BG, Sparks AB, Alferov O, Hong P, Alexeev A, et al. Accurate whole-
490 genome sequencing and haplotyping from 10 to 20 human cells. *Nature*. 2012;487
491 7406:190-5. doi:10.1038/nature11236.
- 492 16. Edge P, Bafna V and Bansal V. HapCUT2: robust and accurate haplotype assembly for
493 diverse sequencing technologies. *Genome Res*. 2017;27 5:801-12.
494 doi:10.1101/gr.213462.116.

- 495 17. Patterson M, Marschall T, Pisanti N, van Iersel L, Stougie L, Klau GW, et al. WhatsHap:
496 Weighted Haplotype Assembly for Future-Generation Sequencing Reads. *J Comput Biol.*
497 2015;22 6:498-509. doi:10.1089/cmb.2014.0157.
- 498 18. Zheng GX, Lau BT, Schnall-Levin M, Jarosz M, Bell JM, Hindson CM, et al. Haplotyping
499 germline and cancer genomes with high-throughput linked-read sequencing. *Nat*
500 *Biotechnol.* 2016;34 3:303-11. doi:10.1038/nbt.3432.
- 501 19. Spies N, Weng Z, Bishara A, McDaniel J, Catoe D, Zook JM, et al. Genome-wide
502 reconstruction of complex structural variants using read clouds. *Nat Methods.* 2017;14
503 9:915-20. doi:10.1038/nmeth.4366.
- 504 20. Bishara A, Moss EL, Kolmogorov M, Parada AE, Weng Z, Sidow A, et al. High-quality
505 genome sequences of uncultured microbes by assembly of read clouds. *Nat Biotechnol.*
506 2018; doi:10.1038/nbt.4266.
- 507 21. Weisenfeld NI, Kumar V, Shah P, Church DM and Jaffe DB. Direct determination of
508 diploid genome sequences. *Genome Res.* 2017;27 5:757-67. doi:10.1101/gr.214874.116.
- 509 22. Mostovoy Y, Levy-Sakin M, Lam J, Lam ET, Hastie AR, Marks P, et al. A hybrid approach
510 for de novo human genome sequence assembly and phasing. *Nat Methods.* 2016;13 7:587-
511 90. doi:10.1038/nmeth.3865.
- 512 23. Hulse-Kemp AM, Maheshwari S, Stoffel K, Hill TA, Jaffe D, Williams SR, et al. Reference
513 quality assembly of the 3.5-Gb genome of *Capsicum annuum* from a single linked-read
514 library. *Hortic Res.* 2018;5:4. doi:10.1038/s41438-017-0011-0.
- 515 24. Elyanow R, Wu HT and Raphael BJ. Identifying structural variants using linked-read
516 sequencing data. *Bioinformatics.* 2017; doi:10.1093/bioinformatics/btx712.

- 517 25. Jones SJ, Haulena M, Taylor GA, Chan S, Bilobram S, Warren RL, et al. The Genome of
518 the Northern Sea Otter (*Enhydra lutris kenyoni*). *Genes* (Basel). 2017;8 12
519 doi:10.3390/genes8120379.
- 520 26. Zhang F, Christiansen L, Thomas J, Pokholok D, Jackson R, Morrell N, et al. Haplotype
521 phasing of whole human genomes using bead-based barcode partitioning in a single tube.
522 *Nat Biotechnol*. 2017;35 9:852-7. doi:10.1038/nbt.3897.
- 523 27. Peters BA, Liu J and Drmanac R. Co-barcoded sequence reads from long DNA fragments:
524 a cost-effective solution for "perfect genome" sequencing. *Front Genet*. 2014;5:466.
525 doi:10.3389/fgene.2014.00466.
- 526 28. Pendleton M, Sebra R, Pang AW, Ummat A, Franzen O, Rausch T, et al. Assembly and
527 diploid architecture of an individual human genome via single-molecule technologies. *Nat*
528 *Methods*. 2015;12 8:780-6. doi:10.1038/nmeth.3454.
- 529 29. Ma ZS, Li L, Ye C, Peng M and Zhang YP. Hybrid assembly of ultra-long Nanopore reads
530 augmented with 10x-Genomics contigs: Demonstrated with a human genome. *Genomics*.
531 2018; doi:10.1016/j.ygeno.2018.12.013.
- 532 30. Li H. Minimap2: pairwise alignment for nucleotide sequences. *Bioinformatics*. 2018;34
533 18:3094-100. doi:10.1093/bioinformatics/bty191.
- 534 31. Mikheenko A, Prjibelski A, Saveliev V, Antipov D and Gurevich A. Versatile genome
535 assembly evaluation with QUAST-LG. *Bioinformatics*. 2018;34 13:i142-i50.
536 doi:10.1093/bioinformatics/bty266.
- 537 32. Earl D, Bradnam K, St John J, Darling A, Lin D, Fass J, et al. Assemblathon 1: a
538 competitive assessment of de novo short read assembly methods. *Genome Res*. 2011;21
539 12:2224-41. doi:10.1101/gr.126599.111.

540

541 **Supplementary Notes**

542

543 **LRTK-SIM**

544 LRTK-SIM was designed to simulate linked-reads generated by the 10X Chromium instrument
545 and Illumina sequencer, which consists of four key steps:

- 546 **1. Generate diploid reference genome of NA12878.** (See Methods in main manuscript.)
- 547 **2. Simulate long DNA fragments.** Assuming the DNA fragment physical coverage was C_F , the
548 total volume of DNA was represented as $V=C_F*L$, where L represented the length of reference
549 genome. Equal physical coverage was assumed for two haplotypes, i.e. $\frac{C_F}{2}$. The start point for
550 each fragment was randomly picked across the reference and its unweighted length is
551 generated from an exponential distribution with mean of μ_{FL} .
- 552 **3. DNA fragment barcoding.** About 4.79 million 16-mer barcode sequences were available in
553 the Long Ranger whitelist. LRTK-SIM generated 'pseudo' partitions with unique barcodes and
554 allocated long DNA fragments to them. The number of fragments per partition was sampled
555 from a Poisson distribution with mean of $N_{F/P}$.
- 556 **4. Simulate Illumina short reads.** LRTK-SIM assumed short reads cover the long DNA
557 fragments uniformly. The number of reads to be generated were calculated as $\frac{C_R \times V}{R_L}$, where R_L
558 is the length for short reads (150bp by default). The insert size for paired-end reads follows a
559 normal distribution with mean of 400bp. The empirical base quality was learned from linked-
560 reads that were sequenced by Illumina HiSeq X and the positions of sequencing errors were
561 selected randomly.

562

563 LRTK-SIM has two advantages: 1. LRTK-SIM is an all-in-one package and implemented in python;
564 it does not rely on any external packages or programs. 2. It explicitly imitates the generation of
565 linked-reads and includes four key parameters: C_F , C_R , μ_{FL} and $N_{F/P}$ to fine-tune modeling of the
566 experimental workflow. LRTK-SIM is speeded up by multithreading and publicly available at
567 <https://github.com/LRTK/LRTK-SIM>.

568

569 **Evaluation of diploid assembly**

570 The performance of assembly was evaluated by QUAST-LG and our in-house programs. The
571 scaffolds were broken into contigs when encountering at least 10 consecutive 'N's. Minimap2 was
572 applied to align contigs against reference genome and QUAST-LG was used to post-process the

573 alignments. Contigs shorter than 500bp and scaffolds shorter than 1kb were removed from
574 evaluation. Contig-aligned blocks were generated by breaking contigs at misassemblies,
575 including relocation, inversion and translocation (according to QUASt-LG).

576

577 Similar to contigs, for calculating scaffold NA50 scaffold-aligned blocks were obtained by breaking
578 scaffolds at contig misjoins. For example, if there are three contigs ordered as $\{a, b, c\}$ in the
579 scaffold, misjoins were classified into four types: 1) Relocation, if the alignment-based order of
580 the contigs was different but on the same chromosome; for example if the contigs were aligned
581 in the order $\{a, c, b\}$ to the hg38 assembly. 2) Inversion, if two connected contigs were in the same
582 order but one of them had reversed orientation in the alignment. 3) Translocation, if two
583 sequences from different chromosomes were merged into adjacent contigs. 4) Indel, if an internal
584 contig such as b was unaligned or removed due to insufficient contig length ($<500\text{bp}$). Indels were
585 not considered misjoins if b was shorter than 200bp or the gap between a and c was within 1000bp
586 of b 's length.

587 **Supplementary Tables**

588

Raw DNA Preparation	Sequenced Library	Sample id	Raw coverage (X)	$\mu_{FL}/W\mu_{FL}$ (kb)	PCR duplication (%)	C_F (X)	C_R (X)
<i>Prep</i> ₁	<i>L</i> _{1L}	NA12878	94	21.6/38.7	53.08	19.3	0.83
<i>Prep</i> ₁	<i>L</i> _{1M}	NA12878	175	22.4/39.7	29.24	117.6	0.54
<i>Prep</i> ₁	<i>L</i> _{1H}	NA12878	192	24.0/41.1	10.92	334	0.27
<i>Prep</i> ₂	<i>L</i> ₂	NA12878	103	79.0/304.3	19.97	123.2	0.41
<i>Prep</i> ₃	<i>L</i> ₃	NA12878	106	99.2/214.5	11.09	958.7	0.07
<i>Prep</i> ₄	<i>L</i> ₄	NA24385	117	92.1/216.9	10.88	1504.6	0.05
<i>Prep</i> ₅	<i>L</i> ₅	NA24385	100	120.8/267.4	18.51	208.4	0.25
<i>Prep</i> ₆	<i>L</i> ₆	NA24385	100	64.2/151.7	12.39	803.3	0.08

589

590

Table S1. Parameters of libraries prepared for NA12878 and NA24385.

Parameters	Linked-Read set	$\mu_{FL}/W\mu_{FL}$ (kb)	N_{FP}	C_F (X)	C_R (X)	C (X)
C_F	C_{F1}	37/75	10	156	0.10	16
	C_{F2}	37/75	10	156	0.27	42
	C_{F3}	37/75	10	156	0.36	56
	C_{F4}	37/75	10	156	0.5	78
C_R	C_{R1}	37/75	10	44	0.36	16
	C_{R2}	37/75	10	117	0.36	42
	C_{R3}	37/75	10	156	0.36	56
	C_{R4}	37/75	10	217	0.26	78

591

592 **Table S2.** Parameters used to generate Linked-Read sets for evaluating the impact of C_F and

593 C_R on assemblies.

Parameters	Linked-Read set	$\mu_{FL}/W\mu_{FL}$ (kb)	N_{FP}	C_F (X)	C_R (X)	C (X)
μ_{FL}	$\mu_{FL1}/W\mu_{FL1}$	37/75	10	156	0.36	56
	$\mu_{FL2}/W\mu_{FL2}$	80/161	10	156	0.36	56
	$\mu_{FL3}/W\mu_{FL3}$	110/221	10	156	0.36	56
	$\mu_{FL4}/W\mu_{FL4}$	200/402	10	156	0.36	56
N_{FP}	N_{FP1}	37/75	1	156	0.36	56
	N_{FP2}	37/75	2	156	0.36	56
	N_{FP3}	37/75	4	156	0.36	56
	N_{FP4}	37/75	8	156	0.36	56
	N_{FP5}	37/75	16	156	0.36	56

594

595 **Table S3.** Parameters used to generate Linked-Read sets for evaluating the impact of μ_{FL} and
596 N_{FP} on assemblies.

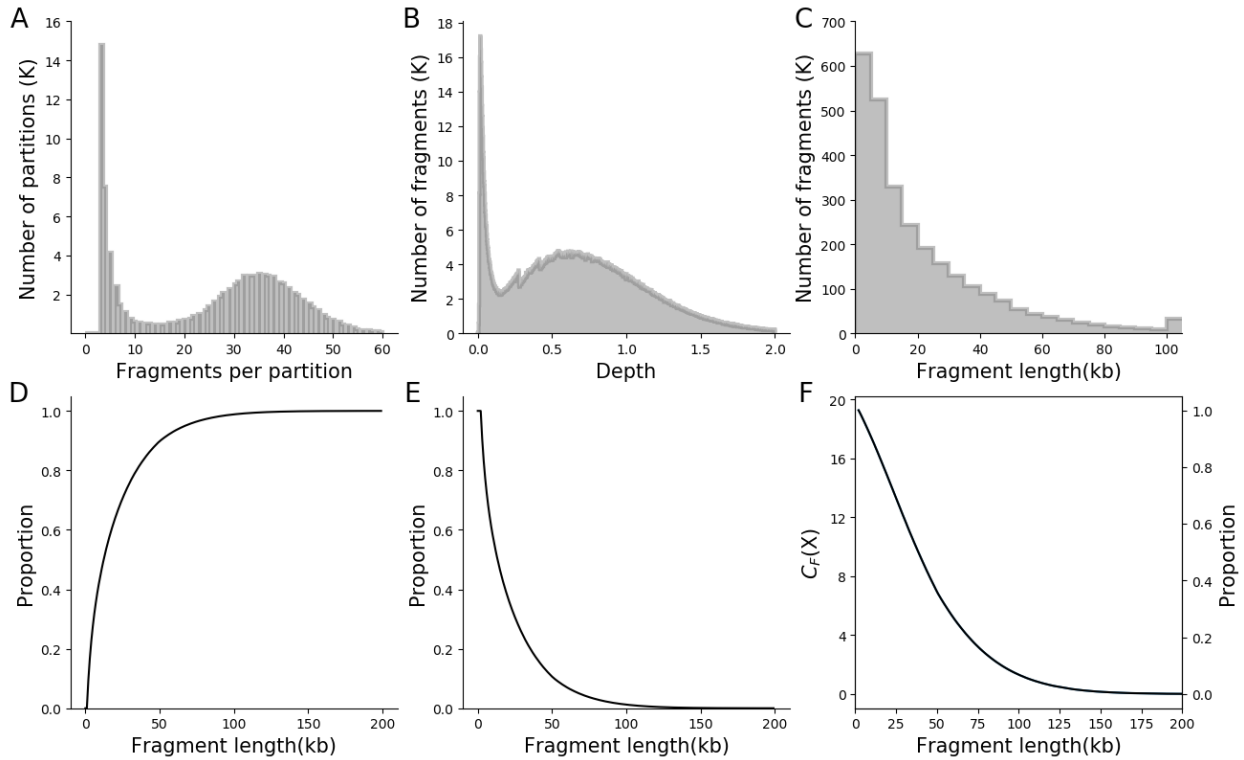
Library	Overall (%)	Diploid regions (%)	Haploid regions (%)	Non-PAR (%)
HGP	91.9%	79.7%	4.59%	88.8%
ASH	91.8%	79.5%	5.26%	88.0%
WFU	91.9%	76.5%	8.59%	-
CHI	91.8%	78.3%	7.50%	87.7%
YOR	91.8%	80.1%	2.27%	-
YORM	91.9%	76.7%	2.68%	-
PR	91.9%	77.2%	7.89%	-

597

598 **Table S4.** Genomic coverage and fraction of contigs in diploid state generated by Supernova2
599 for the seven libraries prepared by 10x Genomics. Non-PAR: non-pseudoautosomal regions of
600 X chromosome. WFU, YOR, YORM, PR are female; HGP, ASH and CHI are male.

601 **Supplementary Figures**

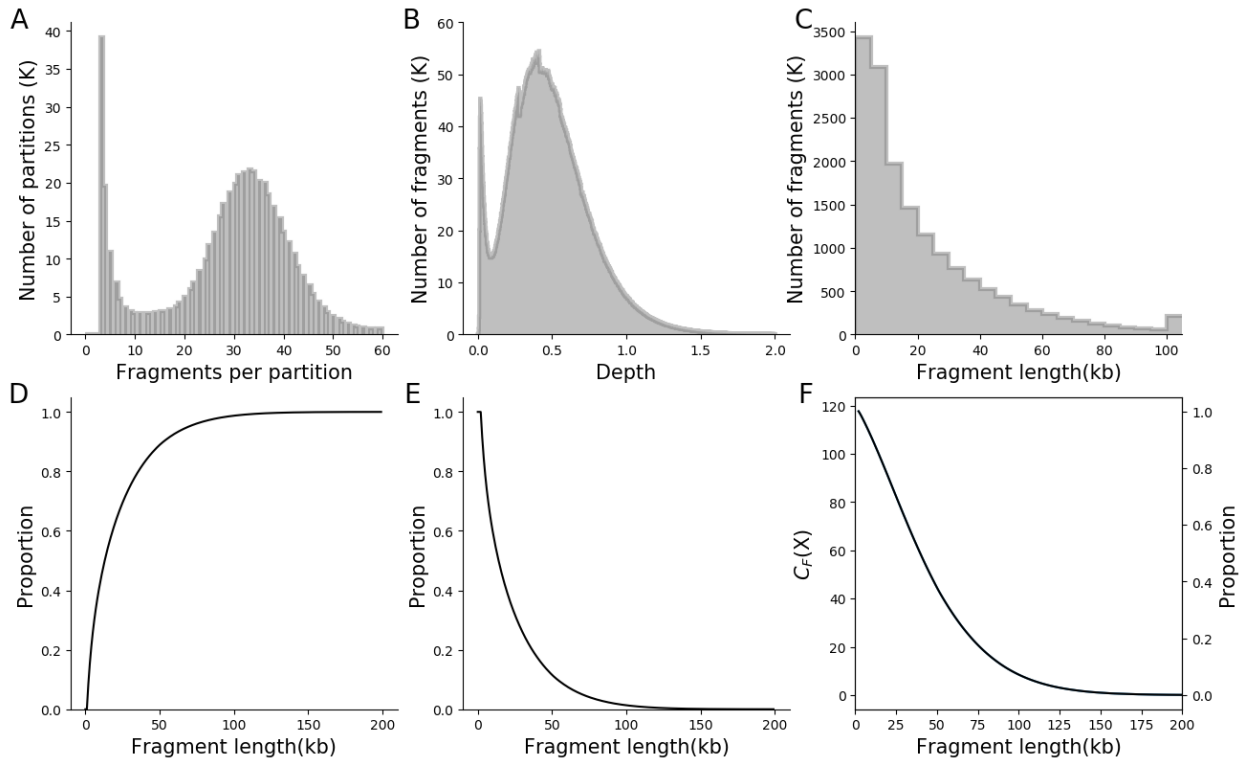
602



603
604

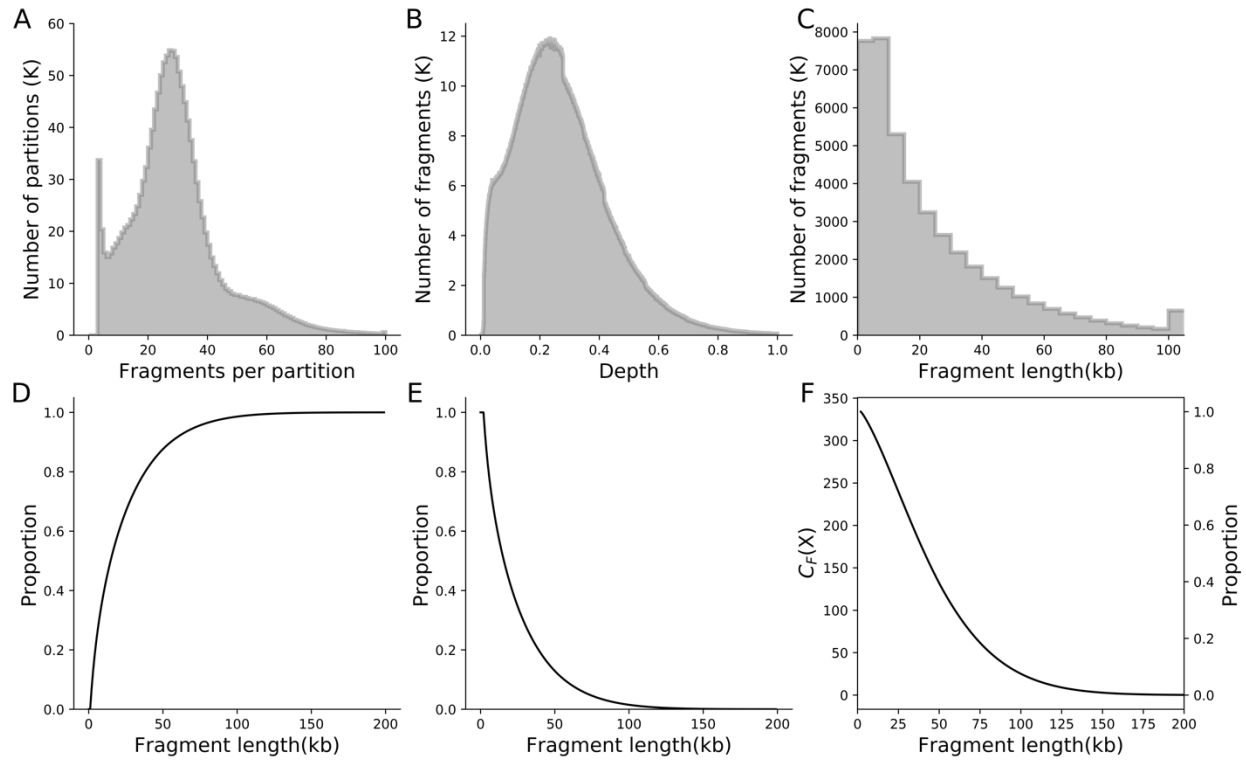
605 **Figure S1. Basic statistics for L_{1L} .** The distributions of **A.** the number of fragments per partition;
606 **B.** sequencing depth per fragment; **C.** probability density function of unweighted fragment lengths;
607 **D.** cumulative density function of unweighted fragment lengths; **E.** reversed cumulative density
608 function of unweighted fragment lengths; **F.** reversed cumulative density function of weighted
609 fragment lengths.

610



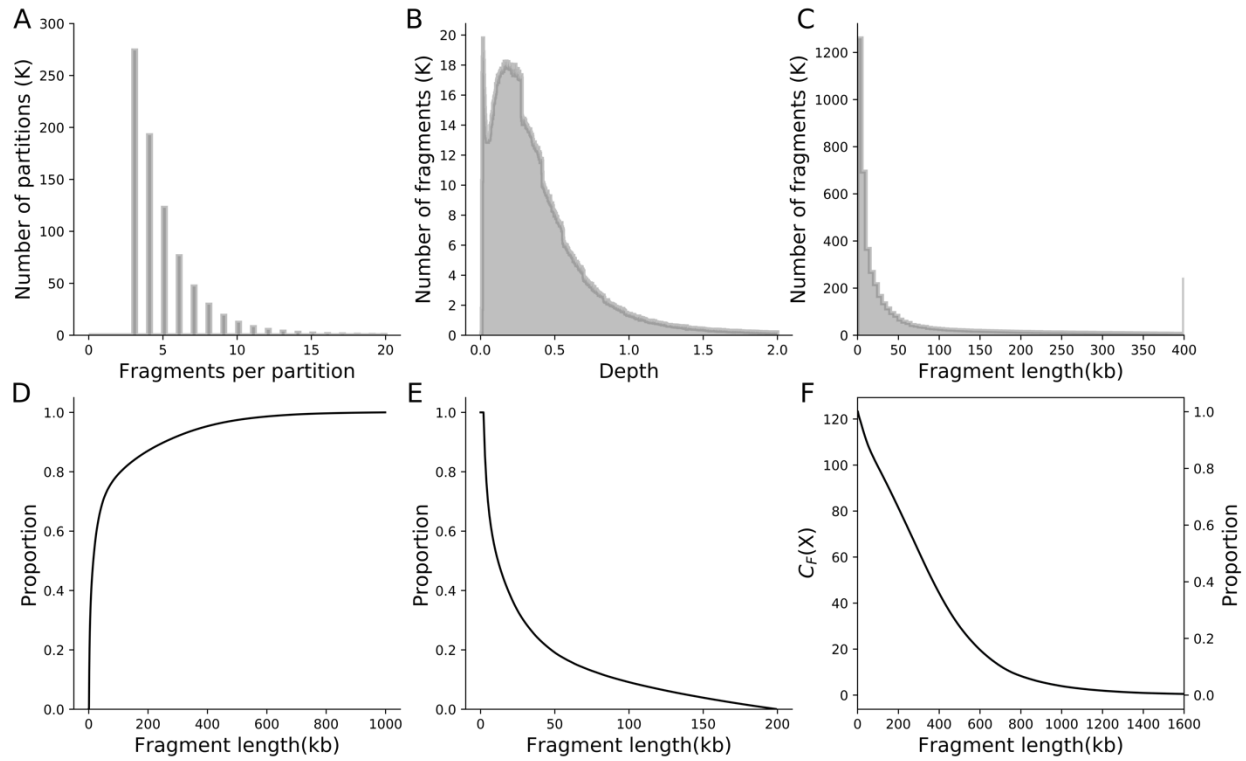
611
612

613 **Figure S2. Basic statistics for L_{1M} .** The distributions of **A.** number of fragments per partition; **B.**
614 sequencing depth per fragment; **C.** probability density function of unweighted fragment lengths;
615 **D.** cumulative density function of unweighted fragment lengths; **E.** reversed cumulative density
616 function of unweighted fragment lengths; **F.** reversed cumulative density function of weighted
617 fragment lengths.



618
619

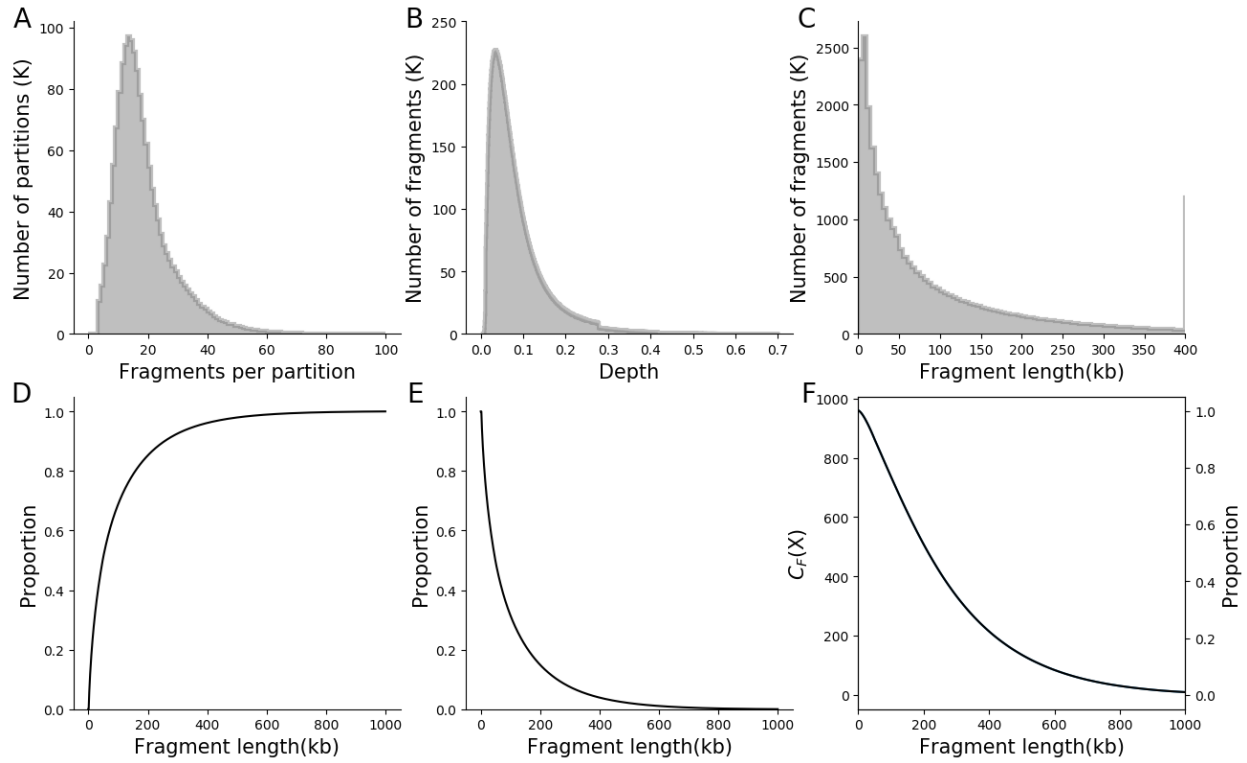
620 **Figure S3. Basic statistics for L_{1H} .** The distributions of **A.** number of fragments per partition; **B.**
 621 sequencing depth per fragment; **C.** probability density function of unweighted fragment lengths;
 622 **D.** cumulative density function of unweighted fragment lengths; **E.** reversed cumulative density
 623 function of unweighted fragment lengths; **F.** reversed cumulative density function of weighted
 624 fragment lengths.



625
626

627 **Figure S4. Basic statistics for L_2 .** The distributions of **A.** number of fragments per partition; **B.**
 628 sequencing depth per fragment; **C.** probability density function of unweighted fragment lengths;
 629 **D.** cumulative density function of unweighted fragment lengths; **E.** reversed cumulative density
 630 function of unweighted fragment lengths; **F.** reversed cumulative density function of weighted
 631 fragment lengths.

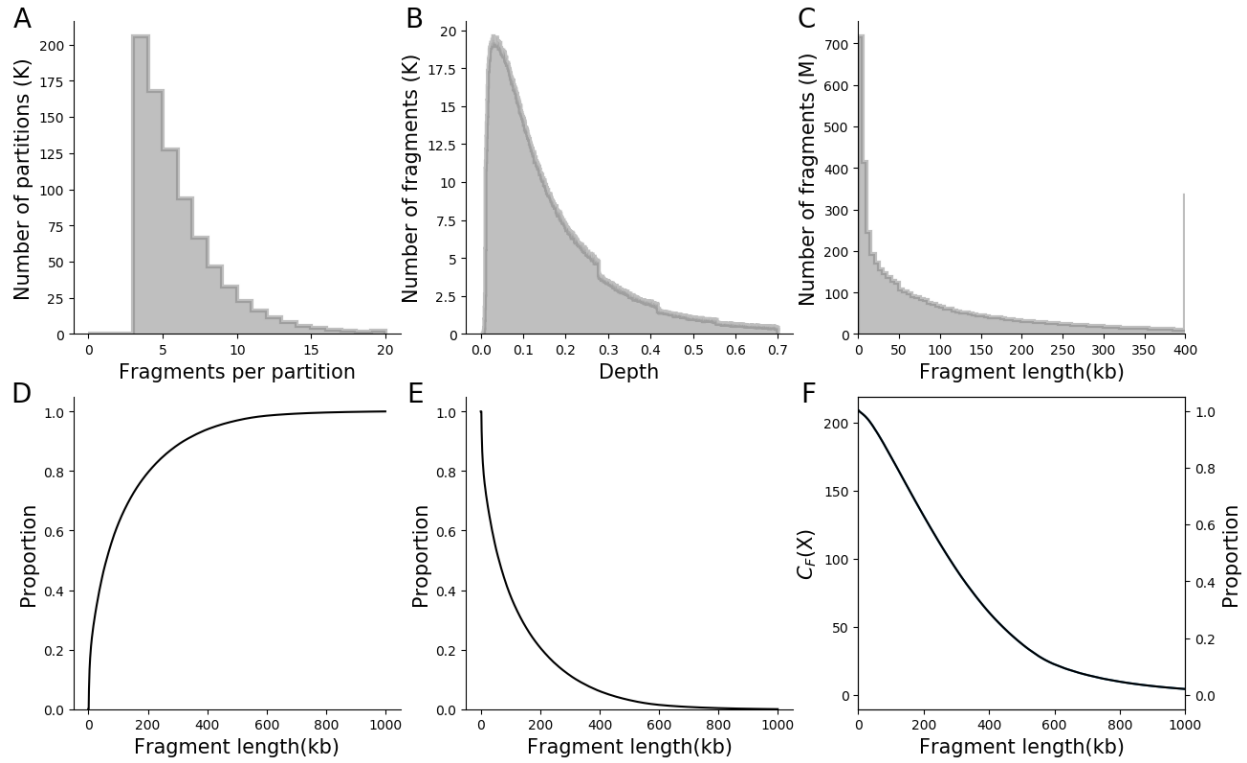
632



633
634

635 **Figure S5. Basic statistics for L_3 .** The distributions of **A.** number of fragments per partition; **B.**
 636 sequencing depth per fragment; **C.** probability density function of unweighted fragment lengths;
 637 **D.** cumulative density function of unweighted fragment lengths; **E.** reversed cumulative density
 638 function of unweighted fragment lengths; **F.** reversed cumulative density function of weighted
 639 fragment lengths.

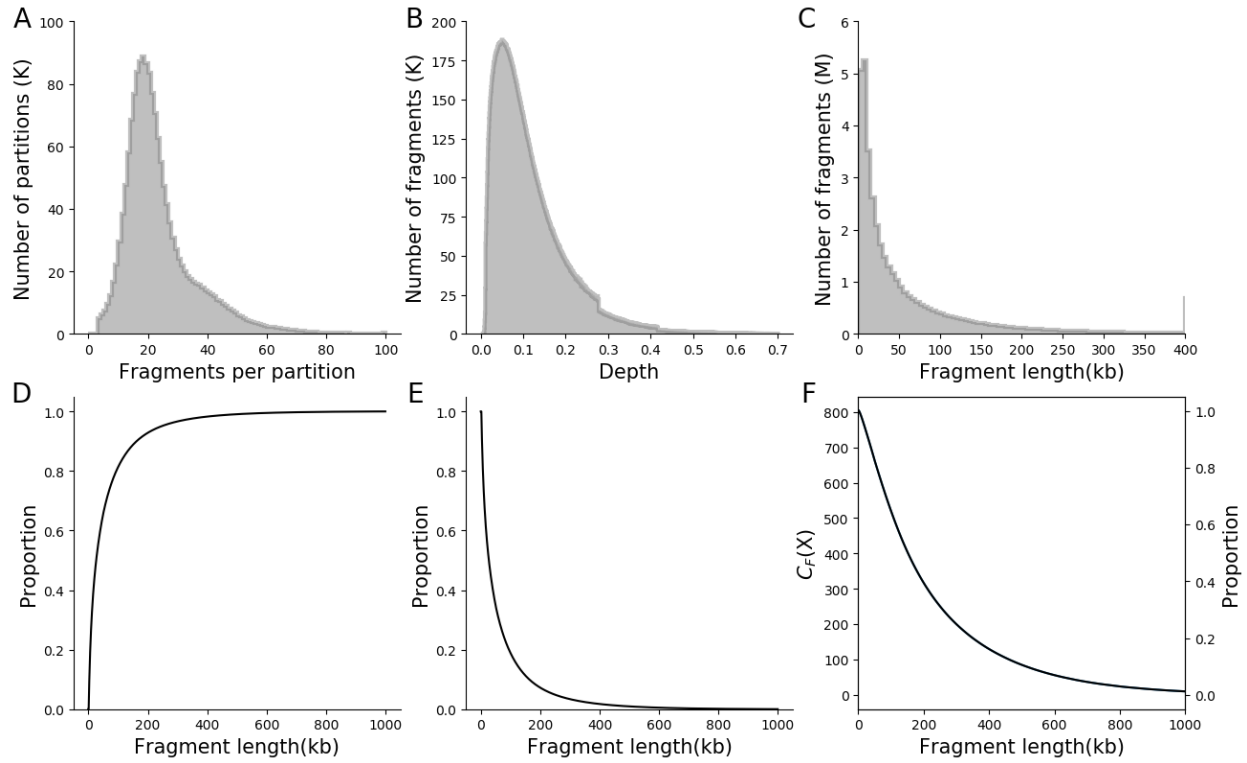
640



641
642

643 **Figure S6. Basic statistics for L_4 .** The distributions of **A.** number of fragments per partition; **B.**
 644 sequencing depth per fragment; **C.** probability density function of unweighted fragment lengths;
 645 **D.** cumulative density function of unweighted fragment lengths; **E.** reversed cumulative density
 646 function of unweighted fragment lengths; **F.** reversed cumulative density function of weighted
 647 fragment lengths.

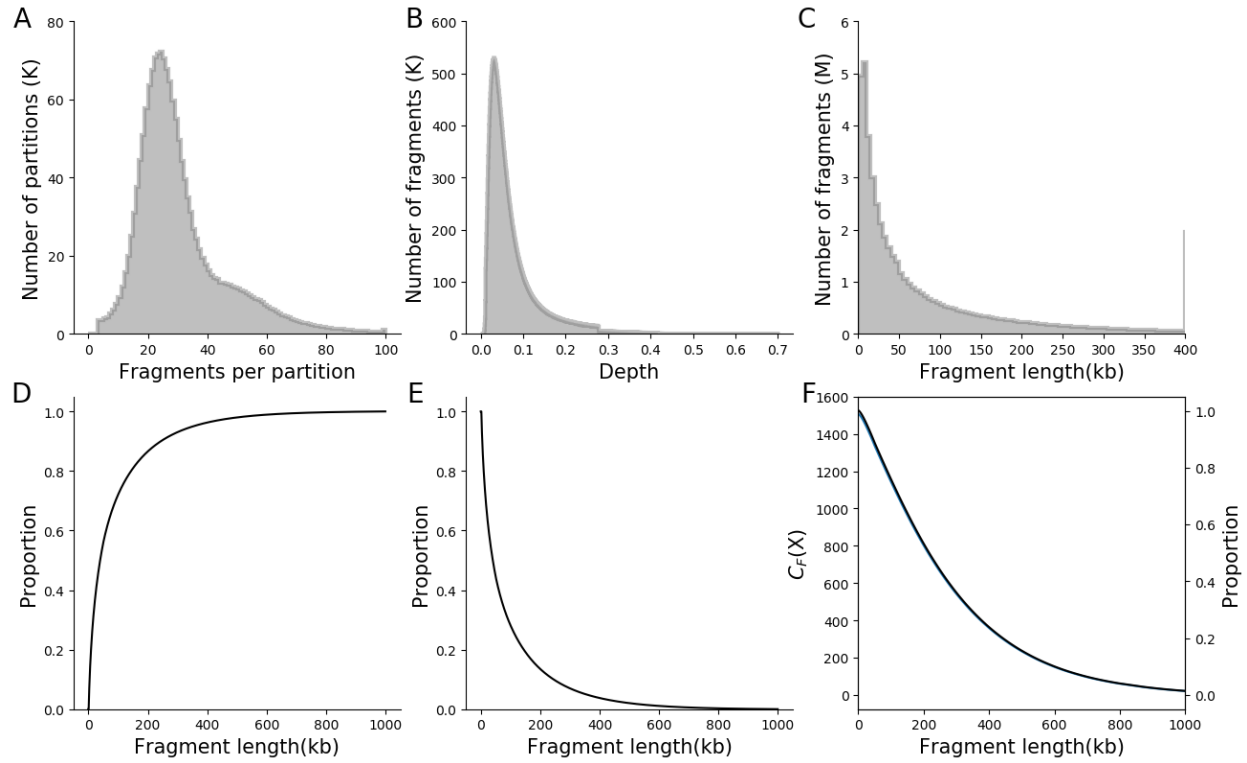
648



649
650

651 **Figure S7. Basic statistics for L_5 .** The distributions of **A.** number of fragments per partition; **B.**
 652 sequencing depth per fragment; **C.** probability density function of unweighted fragment lengths;
 653 **D.** cumulative density function of unweighted fragment lengths; **E.** reversed cumulative density
 654 function of unweighted fragment lengths; **F.** reversed cumulative density function of weighted
 655 fragment lengths.

656



657
658

659 **Figure S8. Basic statistics for L_6 .** The distributions of **A.** number of fragments per partition; **B.**
 660 sequencing depth per fragment; **C.** probability density function of unweighted fragment lengths;
 661 **D.** cumulative density function of unweighted fragment lengths; **E.** reversed cumulative density
 662 function of unweighted fragment lengths; **F.** reversed cumulative density function of weighted
 663 fragment lengths.

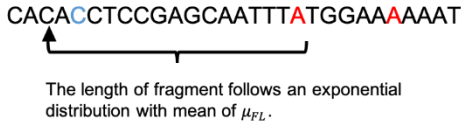
664

1. Generate diploid reference sequences by inserting variants

Reference CACATCTCCGAGCAATTTCTGGAATAAAT
 Haplotype1 CACACCTCCGAGCAATTTATGGAAAAT
 Haplotype2 CACATCTCTGAGGAATTTCTGGAATAAAT

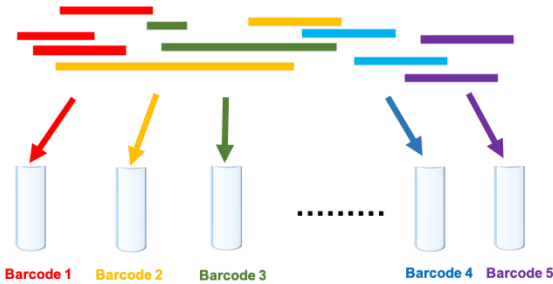
- ✓ Download human reference genome (hg38)
- ✓ Insert SNVs from high-confidence regions of NA12878 from GIAB
- ✓ Insert 1 SNV per 1Kb to low-confidence regions of NA12878

2. Simulate long DNA fragments



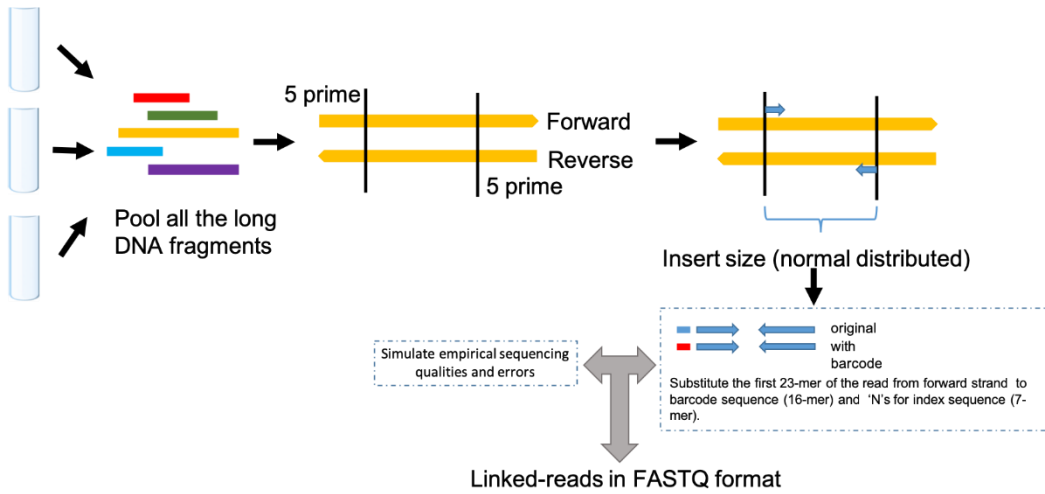
- ✓ Calculate the number of long DNA fragments: $\frac{C_F * L}{\mu_{FL}}$
- ✓ Randomly select the fragment start positions
- ✓ Generate the fragment length from an exponential distribution with mean of μ_{FL}
- ✓ Merge all the simulated fragments from two haplotypes together

3. Randomly allocate long DNA fragments into partitions, each partition is assigned a unique barcode.



- ✓ The average number of fragments per partition is $N_{F/P}$
- ✓ the number of fragments per partition follows a Poisson distribution with mean of $N_{F/P}$.

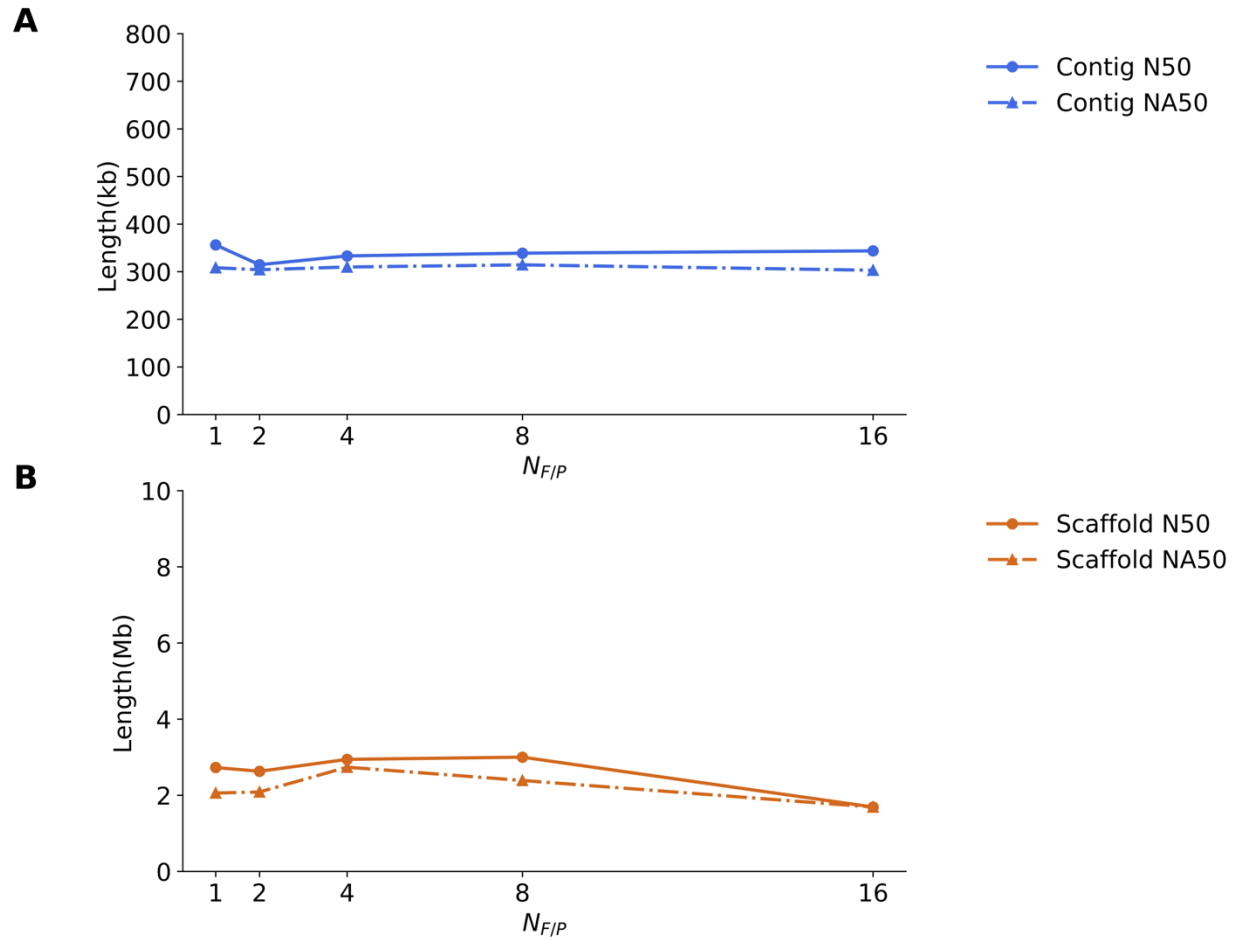
4. Simulate paired-end short reads



5. Repeat step 1 to 4 with different parameters to simulate multiple libraries.

665
666

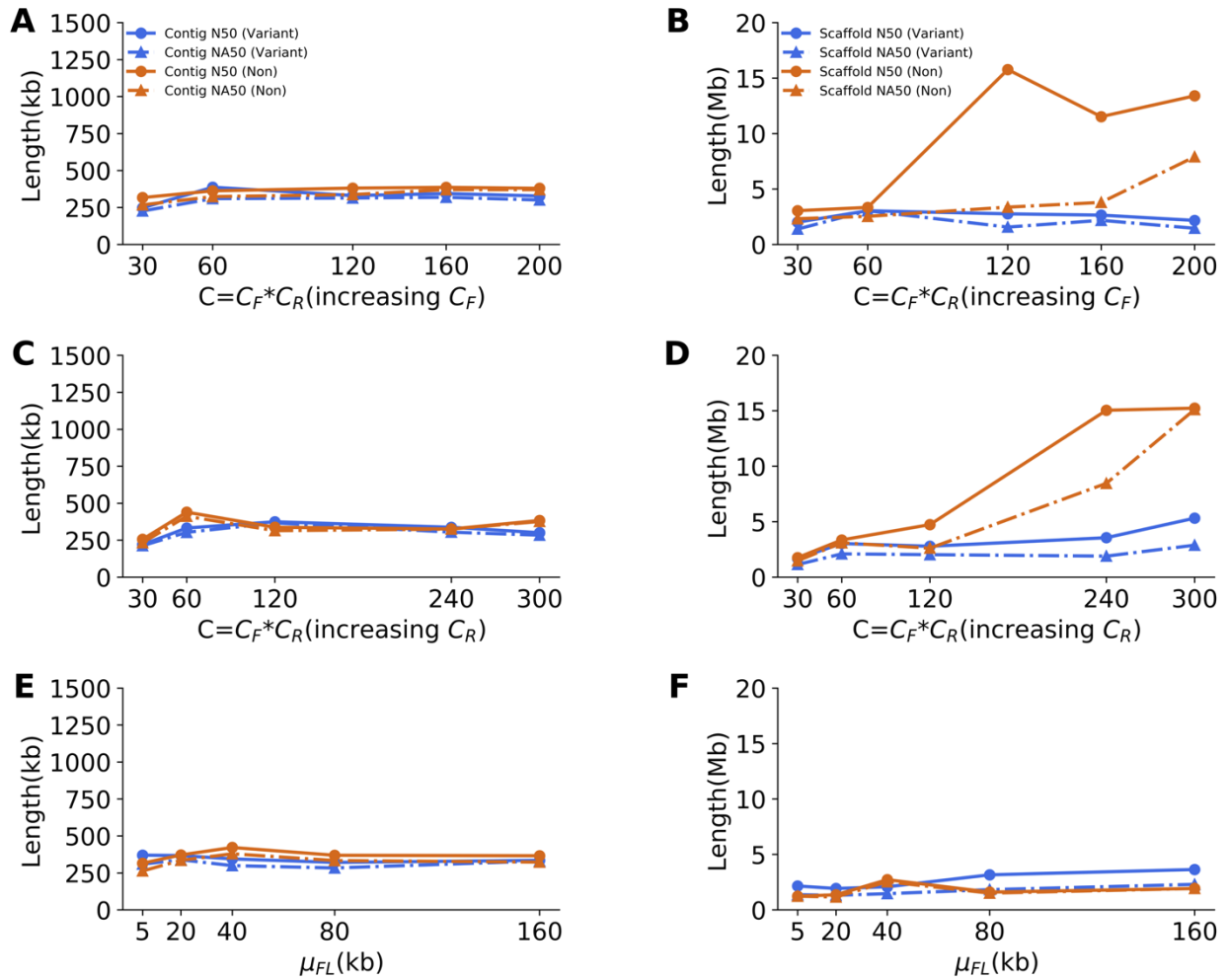
Figure S9. The workflow of LRTK-SIM to simulate linked-reads



667

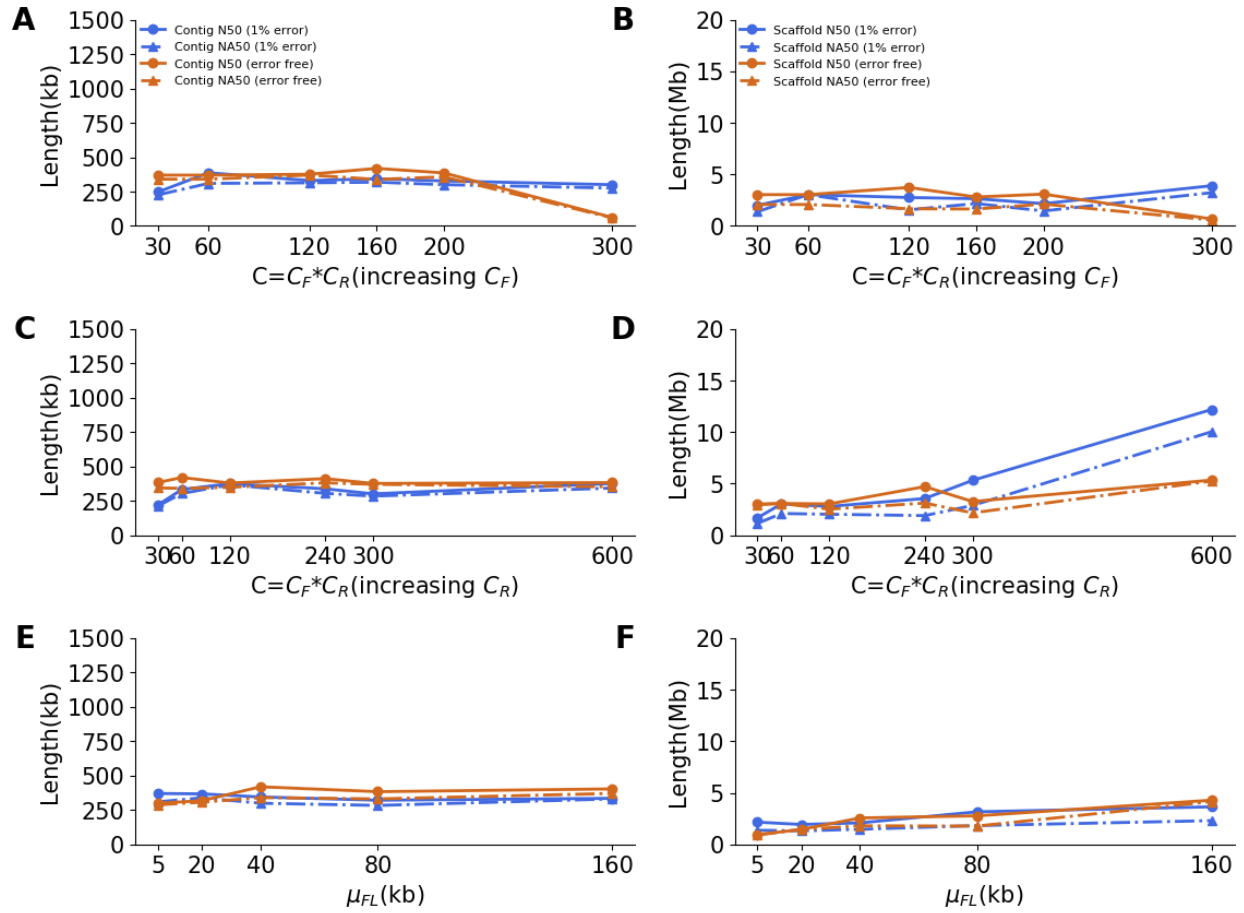
668 **Figure S10.** The effect of $N_{F/P}$ on human diploid assembly of chromosome 19 by Supernova2,

669 where C ($C=60X$; $C_F=300X$ and $C_R=0.2X$) and μ_{FL} ($\mu_{FL}=37\text{kb}$) are fixed.



670
 671
 672
 673

Figure S11. Comparison of assembly qualities from 10x data with and without single nucleotide variants by changing C_F , C_R and μ_{FL} . C_R was fixed to 0.2X in **A** and **B**; C_F was fixed to 300X in **C** and **D**; C_R was fixed 0.2X and C_F was fixed 300X in **E** and **F**.



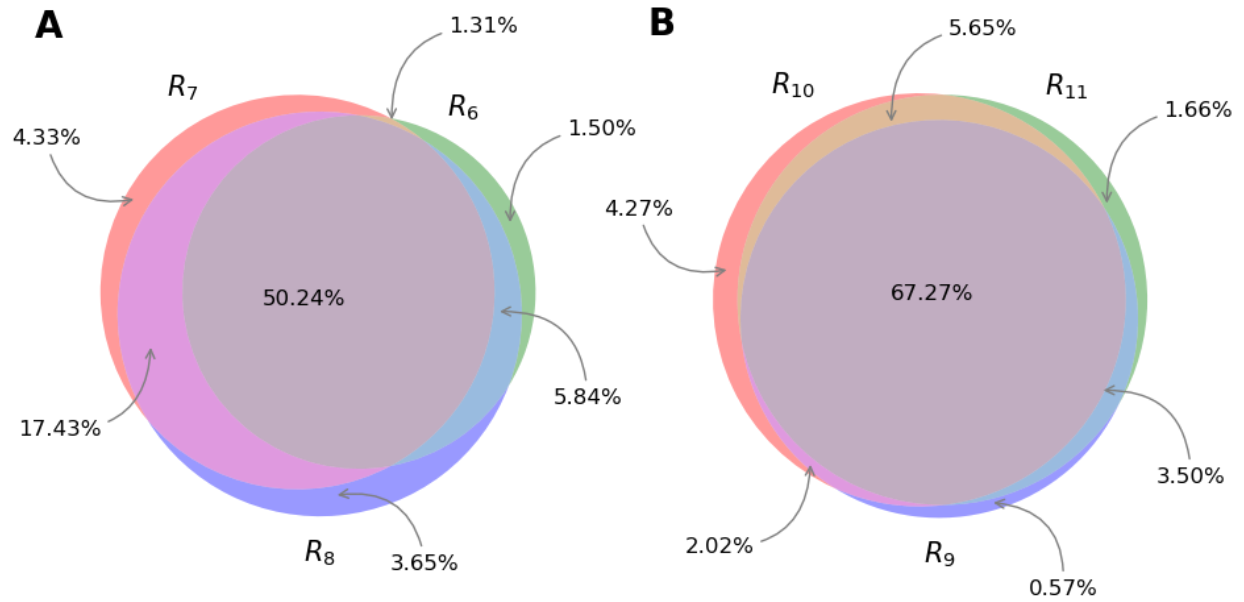
674

675

676

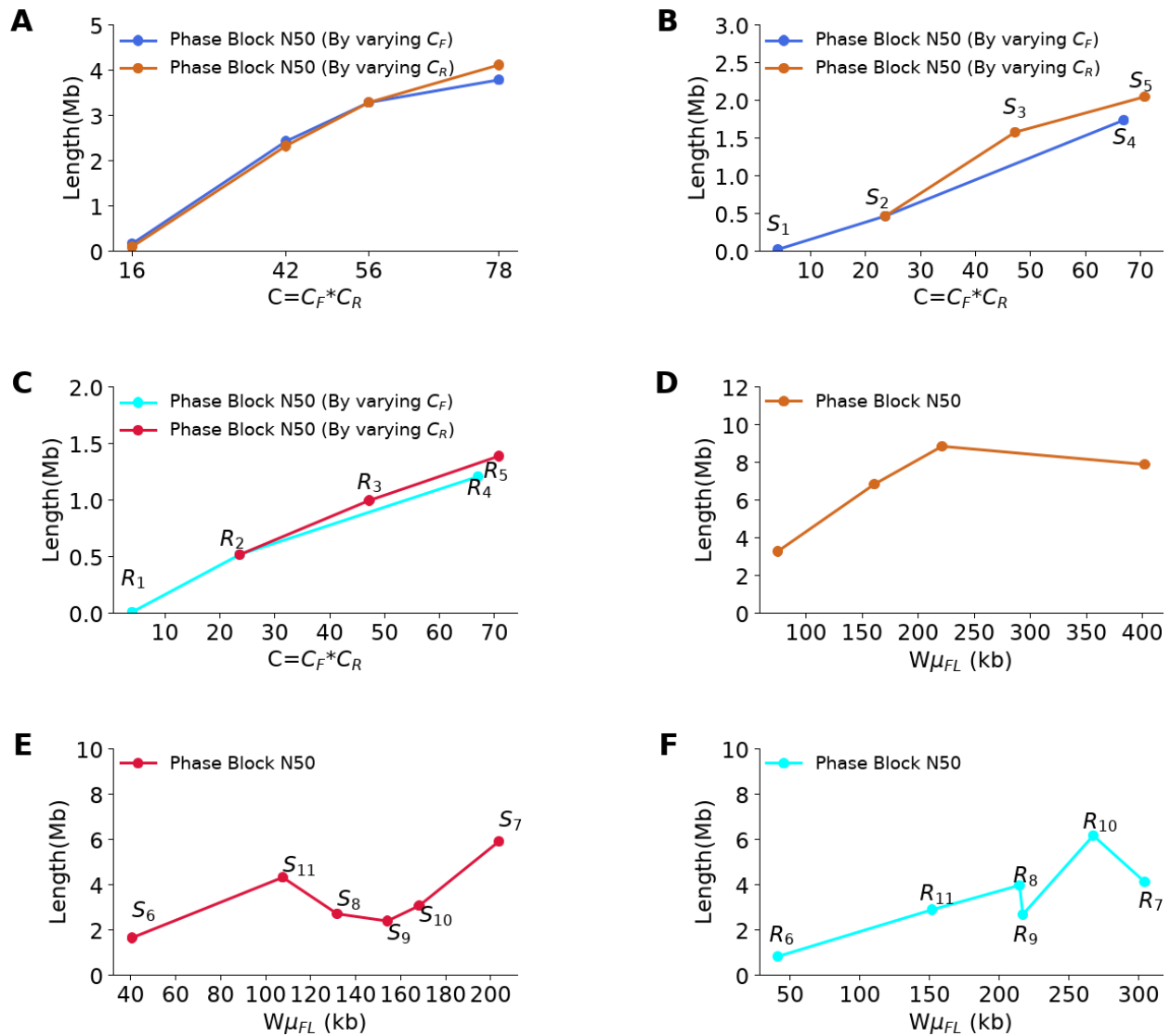
677

Figure S12. Comparison of assembly qualities from 10x data with (1% uniform) and without sequencing error by changing C_F , C_R and μ_{FL} . C_R was fixed to 0.2X in **A** and **B**; C_F was fixed to 300X in **C** and **D**; C_R was fixed 0.2X and C_F was fixed 300X in **E** and **F**.



678
679
680
681
682

Figure S13. Overlaps of diploid regions for the three libraries from the same sample. Diploid regions for NA12878 (A) and NA24385 (B). The percentages denote the proportion of genome is diploid.



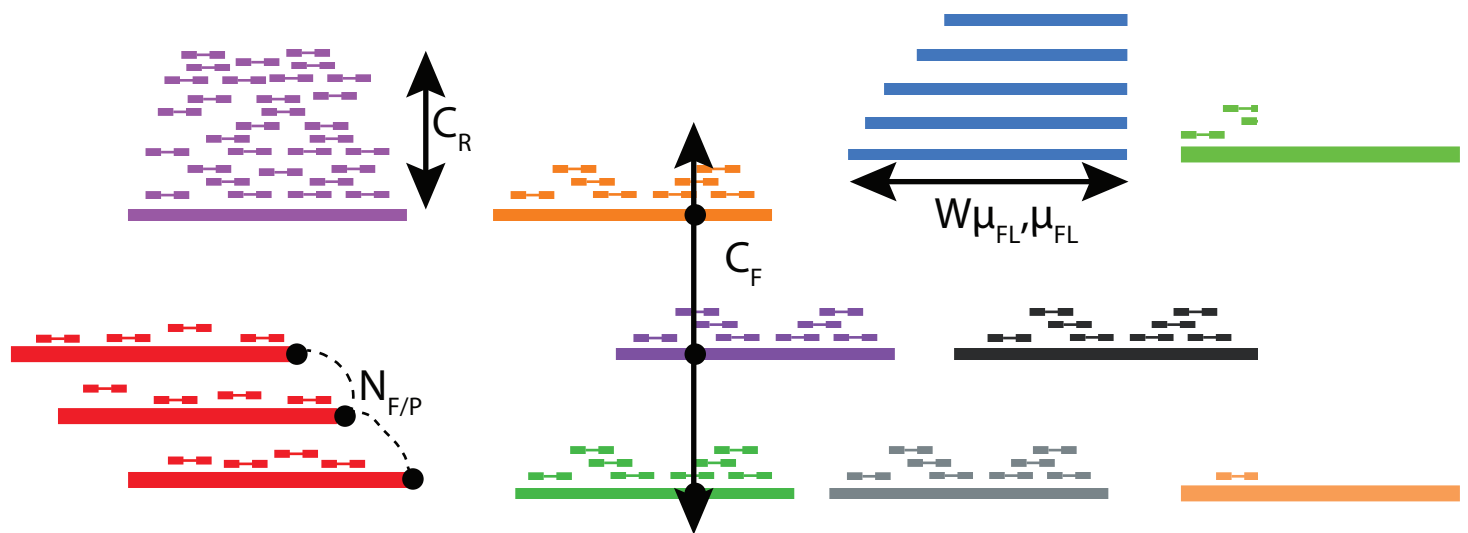
683
684

685 **Figure S14.** Phase block N50s as a function of different parameter combinations. **A.** simulated
686 Linked-Reads with predefined parameters by changing C_F and C_R (**Table S4**); **B.** simulated
687 Linked-Reads with matched parameters of real linked-read sets (**Table S2**) by changing C_F and
688 C_R ; **C.** real Linked-Read sets (**Table S2**) by changing C_F and C_R ; **D.** simulated Linked-Read sets
689 (**Table S3**) with different $W\mu_{FL}$; **E.** simulated Linked-Read sets with matched parameters (**Table**
690 **S3**) with real Linked-Read sets as $C=56X$; **F.** real Linked-Read sets with $C=56X$ (**Table S3**).

Table

Linked- reads set	Overall (%)	Diploid regions (%)	Haploid regions (%)	Non-PAR (%)	Total contig length (contig>500bp)	Length of contigs from megabubble (contig>500bp)	Percentage (%)
R_6	91.9	58.9	27.7	-	5,632,483,053	3,758,345,846	66.73
R_7	91.1	73.3	11.3	-	5,613,140,437	4,668,186,478	83.17
R_8	91.7	77.2	9.2	-	5,635,127,471	4,896,821,850	86.90
R_9	91.3	73.4	12.2	85.9	5,637,615,919	4,438,175,621	78.72
R_{10}	91.7	79.2	5.8	79.9	5,749,001,471	4,793,226,150	83.37
R_{11}	91.7	78.1	7.9	87.6	5,677,566,094	4,723,083,367	83.19

Table 1. Genomic coverage of contigs generated by Supernova2. Non-PAR: non-pseudoautosomal regions of X chromosome. R_6 , R_7 and R_8 are female; R_9 , R_{10} and R_{11} are male.

**Parameter**

$N_{F/P}$ = Number of fragments per partition

μ_{FL} = Mean fragment length

$W\mu_{FL}$ = Weighted mean fragment length

C_R = Read coverage per fragment

C_F = Physical (fragment) coverage

C = total coverage

Typical values

10 - 100

μ_{FL} = 10-100kb

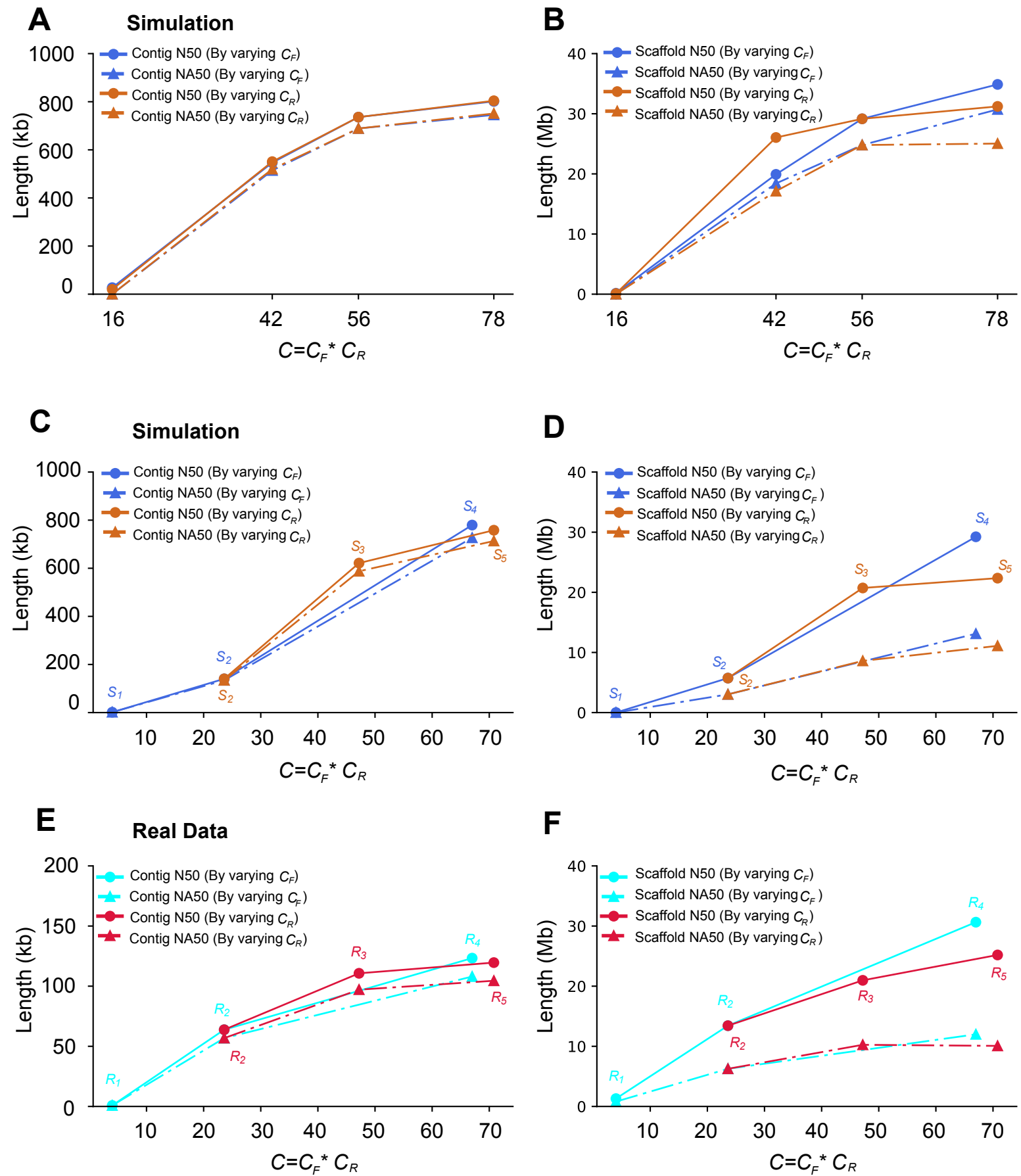
$W\mu_{FL}$ = 20-400kb

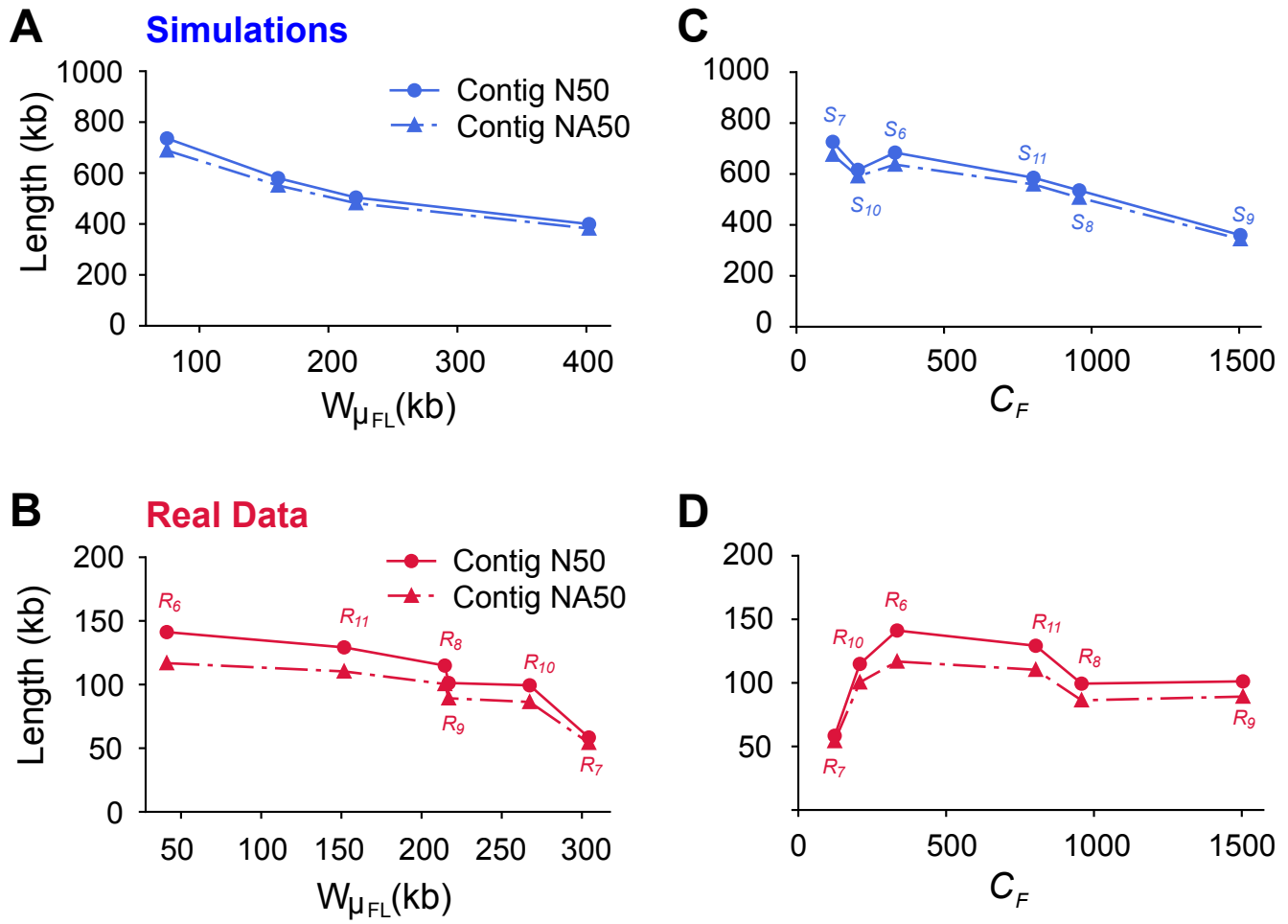
C_R = 0.1x - 0.4x

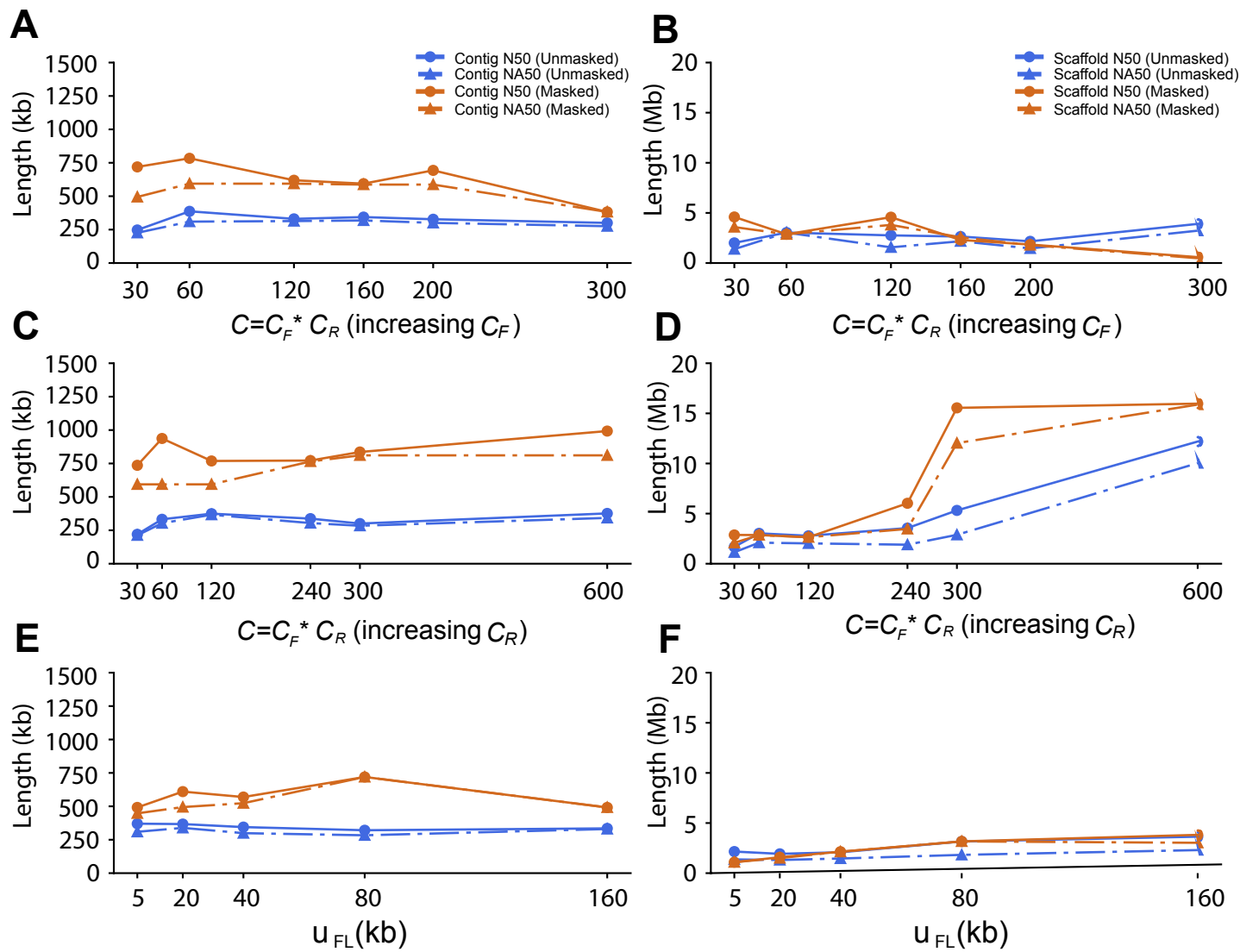
C_F = 200x - 1000x

$C = C_R * C_F = 40x - 80x$

Linked-read set R (Real) / S (Simulated)	Sequenced Library	μ_{FL} (kb)	$W\mu_{FL}$ (kb)	C_F (X)	C_R (X)	C (X)
R_1 / S_1	L_{1L}	21.6	38.6/35.7	19	0.2	4
R_2 / S_2	L_{1M}	22.4	39.7/37.4	117	0.2	24
R_3 / S_3	L_{1M}	22.4	39.7/36.8	117	0.4	48
R_4 / S_4	L_{1H}	24.0	41.1/40.7	334	0.2	67
R_5 / S_5	L_{1M}	22.4	39.7/36.8	117	0.6	72
R_6 / S_6	L_{1H}	24.0	41.1/40.6	334	0.17	56
R_7 / S_7	L_2	79.0	304.3/131.8	123	0.45	56
R_8 / S_8	L_3	99.2	214.5/168.3	958	0.058	56
R_9 / S_9	L_4	92.1	216.9/154.1	1504	0.036	56
R_{10} / S_{10}	L_5	120.8	267.4/203.7	208	0.27	56
R_{11} / S_{11}	L_6	64.2	151.7/107.6	803	0.07	56









Click here to access/download
Supplementary Material
Supplementary Material.docx





DEPARTMENT OF PATHOLOGY
DEPARTMENT OF GENETICS
STANFORD UNIVERSITY SCHOOL OF MEDICINE
STANFORD, CA 94305-5324

Stanford, March 20, 2019

To: GigaScience Editors

Dear Editors,

We are pleased to submit our comprehensive study on *de novo* human genome assembly as a Data Note to GigaScience. *De novo* assembly has received renewed attention for human genomes due to the availability of long-read and Linked-Read approaches. While long-read approaches will remain prohibitively expensive in the foreseeable future and only useful for highly specialized applications, linked-read approaches are cost-effective for larger human cohorts. We therefore explored the experimental and computational parameter space for 10x-based linked read assemblies with Supernova2, the only currently available *de novo* assembler that makes use of linked reads data to produce a diploid assembly.

Beyond the results, which will be useful for a broad audience of scientists who are sequencing human personal genomes, we generated two resources and therefore suggest that our paper clearly fits the purpose of GigaSciences' Data Note. (1) We generated extensive and very deep sequence data on two reference cell lines, NA128787 and NA24385, that will be useful for methods developers in assembly and variation detection. (2) We developed the Linked-Read data simulator, LRTK-SIM, which allows software and applications developers to generate highly realistic linked-read data from a template reference genome.

Linked-Read data sets are still rare but given the potential of the approach and its cost-effectiveness we believe that we are addressing a research direction whose importance will only grow in the future. As we are the first to comprehensively address *de novo* assembly with Linked-Reads, we believe our study will have considerable impact. We hope you will find it sufficiently compelling to send it out for review.

Sincerely,

A handwritten signature in blue ink that reads "Arend Sidow".

Arend Sidow, Ph.D.
Professor of Pathology and of Genetics
SUMC R353
Stanford, CA 94305-5324

arend@stanford.edu
650-498-7024 (ph)
<http://www.sidowlab.org>
<http://jimb.stanford.edu>